สารลดแรงตึงผิวเฉพาะทางในสารหล่อลื่นสำหรับอุตสาหกรรมไมโครอิเล็กทรอนิกส์

นางสาวชื่นกมล คงเผ่า

วิทยานิพนธ์นี้เป็นส่วนหนึ่งของการศึกษาตามหลักสูตรปริญญาวิทยาศาสตรมหาบัณฑิต
สาขาวิชาปิโตรเคมีและวิทยาศาสตร์พอลิเมอร์
คณะวิทยาศาสตร์ จุฬาลงกรณ์มหาวิทยาลัย
ปีการศึกษา 2560

FUNCTIONAL SURFACTANTS IN LUBRICANT FOR MICROELECTRONIC INDUSTRY

Miss Chuenkamol Khongphow

A Thesis Submitted in Partial Fulfillment of the Requirements
for the Degree of Master of Science Program in Petrochemistry and Polymer Science
Faculty of Science
Chulalongkorn University
Academic Year 2017

Thesis Title	FUNCTIONAL SURFACTANTS IN LUBRICANT FOR MICROELECTRONIC INDUSTRY
By	Miss Chuenkamol Khongphow
Field of Study	Petrochemistry and Polymer Science
Thesis Advisor	Assistant Professor Sukkaneste Tungasmita, Ph.D.
Thesis Co-Advisor	Duangamol Tungasmita, Ph.D.

Accepted by the Faculty of Science, Chulalongkorn University in Partial Fulfillment of the Requirements for the Master's Degree

.....Dean of the Faculty of Science

(Professor Polkit Sangvanich, Ph.D.)

THESIS COMMITTEE

.....Chairman

(Assistant Professor Rattachat Mongkolnavin, Ph.D.)

.....Thesis Advisor

(Assistant Professor Sukkaneste Tungasmita, Ph.D.)

.....Thesis Co-Advisor

(Duangamol Tungasmita, Ph.D.)

.....Examiner

(Assistant Professor Pornapa Sujaridworakun, Ph.D.)

.....External Examiner

(Chakkrit Supavasuthi)

ชื่นกมล คงเผ่า : สารลดแรงตึงผิวเฉพาะทางในสารหล่อลื่นสำหรับอุตสาหกรรมไมโครอิเล็กทรอนิกส์ (FUNCTIONAL SURFACTANTS IN LUBRICANT FOR MICROELECTRONIC INDUSTRY) อ.ที่ปรึกษาวิทยานิพนธ์หลัก: ผศ. ดร.สุคคเณศ ตุงคะสมิต, อ.ที่ปรึกษาวิทยานิพนธ์ร่วม: ดร.ดวงกมล ตุงคะสมิต, 74 หน้า.

สารลดแรงตึงผิวเฉพาะทางที่ทำหน้าที่เป็นสารเติมแต่งถูกเพิ่มลงในสารหล่อลื่นมาตรฐานพื้นฐานไกลคอลได้รับการศึกษาและปรับให้เหมาะสมเพื่อลดและป้องกันพื้นผิวของหัวอ่านเขียนที่มีสมบัติเป็นแม่เหล็กจากการทับถมกันของสิ่งปนเปื้อนในระหว่างกระบวนการขัด จากผลของกล้องจุลทรรศน์แบบส่องกราด (เอสอีเอ็ม) ที่ติดตั้งเครื่องวิเคราะห์เชิงพลังงาน (อีดีเอส) วิเคราะห์ได้ว่า สิ่งปนเปื้อนนั้นคืออนุภาคบิสมัส (บีไอ) ที่หลุดออกมาจากแผ่นขัดในระหว่างกระบวนการขัดเนื่องมาจากการสึกหรอ ซึ่งสารลดแรงตึงผิวที่ถูกเลือกแสดงผลในการลดและปกป้องการทับถมกันของสิ่งปนเปื้อนโดยการสร้างไมเซลล์ที่ความเข้มข้นมากว่าค่าความเข้มข้นวิกฤตของไมเซลล์ ในงานวิจัยพบว่าพอลิเอธอกซิเลท แอลกอฮอล์ (พีอีเอแอล) และ ควอเทอร์นารี เอมีน (คิวเอ) สามารถสร้างไมเซลล์ได้ในสารหล่อลื่นมาตรฐานที่ความเข้มข้น 1เปอร์เซ็นต์โดยมวล พอลิเอธิลีน ซอร์บิทอล มอนอลอเรท (พีโอ) สามารถปกป้องพื้นผิวโดยหมู่ฟังก์ชันออกซีเอธิลีนภายในโมเลกุลที่การเติมลงไป 0.2 เปอร์เซ็นต์โดยมวล สมบัติและประสิทธิภาพของสารหล่อลื่นที่ถูกปรับปรุงขึ้นวัดค่าการเปลี่ยนแปลงความต้านทานในสนามแม่เหล็กจากการทดสอบควอไซต์-สเตติก สารหล่อลื่นที่ถูกปรับปรุงขึ้นมีการกระจายตัวของความผิดพลาดของสไลเดอร์ต่ำกว่าสารหล่อลื่นมาตรฐาน นอกจากนี้โพเทนทิโอไดนามิก โพลาไรเซชันให้ผลบ่งชี้ว่าสารหล่อลื่นที่ถูกปรับปรุงขึ้นโดยการเติมสารลดแรงตึงผิวให้ผลดีกว่าสารล่อลื่นมาตรฐานถึง 300 เปอร์เซ็นต์ในกรณีของการป้องกันการกัดกร่อนในระหว่างกระบวนการขัด ดังนั้นสารลดแรงตึงผิวเหล่านี้สามารถทำงานได้ทั้งในฐานะสารเติมแต่งป้องกันการปนเปื้อนและสารเติมแต่งป้องกันการกัดกร่อน นอกจากนี้สารหล่อลื่นที่ถูกปรับปรุงขึ้นเหล่านี้ยังให้เวลาในการขัดและสมบัติทางกายภาพอื่น ๆ ตรงตามความต้องการในการผลิตสไลเดอร์

สาขาวิชา ปิโตรเคมีและวิทยาศาสตร์พอลิเมอร์ ลายมือชื่อนิสิต .....

ปีการศึกษา 2560 ลายมือชื่อ อ.ที่ปรึกษาหลัก .....

ลายมือชื่อ อ.ที่ปรึกษาร่วม .....

5771961823 : MAJOR PETROCHEMISTRY AND POLYMER SCIENCE
KEYWORDS: SURFACTANT / LUBRICANT / MAGNETIC RECORDING HEAD / LAPPING PROCESS

CHUENKAMOL KHONGPHOW: FUNCTIONAL SURFACTANTS IN LUBRICANT FOR MICROELECTRONIC INDUSTRY. ADVISOR: ASST. PROF. SUKKANESTE TUNGASMITA, Ph.D., CO-ADVISOR: DUANGAMOL TUNGASMITA, Ph.D., 74 pp.

The functional surfactants, as the additional additives in the standard glycol-based lubricant were studied and optimized to reduce and protect the surface of the magnetic read/write head from deposited contaminants during the lapping processes. The scanning electron microscopy (SEM) and energy-dispersive x-ray spectroscopy (EDS) results identified that the black contamination was bismuth (Bi) particles, came out from lapping plate during the lapping process due to wear. Selected surfactants exhibited the results in reduce and prevent the deposition of contaminants by forming the micelle beyond their critical micelle concentration (CMC) values. We found that both polyethoxylate alcohol (PEAL) and quaternary amines (QA) can form their micelle in glycol-based lubricant at the ratio of 1 %wt. Polyoxyethylene sorbitan monolaurate (PO) can protect the surface by its oxyethylene groups group at the 0.2 %wt in based lubricant. The characteristics and performances of modified lubricants were measured the change in magnetoresistive resistance value (%DMRR) from quasi-static test (QST). The modified lubricants had minor distribution failure of slider lower than standard lubricant. Moreover, the potentiodynamic polarization measurement results indicated that additional surfactant can also yield almost 300% better performances than the standard lubricant in term of corrosion protection during lapping processes. Thus, these surfactants can function both as the contamination protective additive and as anti-corrosion additive. These modified lubricants can also keep the lap time and other physical performances to match the fabrication requirements.

Field of Study:	Petrochemistry and Polymer Science	Student's Signature	.....
		Advisor's Signature	.....
Academic Year:	2017	Co-Advisor's Signature	.....

ACKNOWLEDGEMENTS

I would like to give my sincere thankfulness and appreciation to my advisor, Assistant Professor Dr. Sukkanest Tungasmita and co-advisor, Dr. Duangamol Tungasmita, who helped me fulfilled my thesis, understood my thinking ways, helped me when I have problems about research and writing thesis, tried to explain the theoretical information and other knowledge in general ways, and enlightened me on the obstacle when I need along my master study and research for whole study.

I would like to gratefully thank to the Western Digital (Thailand) Company Limited, for the all of supporting on this research. Furthermore, I would like to thank all the knowledge, and more working. Then, I would like to give my gratitude to Mr.Chakkrit Supavasuthi for suggestion for this thesis and teach me how to adjust myself for industrial work. I would like to be grateful to Mr.Benjie L. Fernandez and team for all help, supporting and knowledge of final lapping process.Moreover, many thankful to Miss Laddawan Supadee and her team for the knowledge, teaching me to analyze the data and supporting the experiment.I would like to give my gratitude to the chairman, Asst. Prof. Dr. Rattachat Mongkolnavin and member of this thesis committee, Asst. Prof Dr. Pornapa Sujaridworkun, for all their kindness, comment and useful advice in the research.

I have to express my profound gratitude to the supports from Chulalongkorn University Graduate School Thesis Grant, Chulalongkorn University, Thailand.

I would like to thank the DT lab member for their kindness and friendliness over the time. Their sufficient research facilities help me achieved my project.

Finally, I gratefully thank my parents and my friends for providing and supporting me and continuous encouragement throughout the master research life.

CONTENTS

Page

Page

Page

LIST OF FIGURES

Page

LIST OF TABLES

Page

LIST OF ABBREVIATIONS

ABS	Air bearing surface
Å	Angstrom unit
COF	Coefficient of friction
i_{corr}	Corrosion current density
E_{corr}	Corrosion potential
cps/eV	Counts per second per electron-volt
CMC	Critical micelle concentration
°C	Degree Celsius
EDX	Energy-dispersive X-ray spectroscopy
HDD	Hard disk drive
IrMn	Iridium-manganese
MRR	Magneto Resistive Resistance
µS/cm	Microsiemens/ centimeter
mM	Millimolar
M	Molar
nA	Nanoampere
%wt	Percent by weight
%ΔMRR	Percent delta *magneto Resistive Resistance*
QST	Quasi Static Test
SEM	Scanning electron microscope
SL	Standard lubricant
TBN	Total base number

CHAPTER I

INTRODUCTION

1.1 Introduction

Microelectronics has been involved every feature of modern life. We cannot explain which the world does not have computers, notebook, televisions, mobile phones, etc. Recently, microelectronics technology continues to the central nerve of the modern world. Hard disk drives (HDD) have been a main of empowerment electronic data storage technology [1]. The manufacturing process of HDD has been developed by the demand for high recording data. Lapping process is a common process in HDD manufacturing to produce desired surface roughness, dimension, surface topography as well as magnetic property of read-write head (slider) that matched the design criteria and can be assembled to products.

In final lapping process, the standard glycol-based lubricant (SL) was normally used to reduce the damages and defects due to the friction and heat at the contact surface between the specimen and the lapping plate. The flow of lubricant can also help to remove debris out from the contact surface during the lapping process. However, debris and particles of removed materials can re-deposit back on the surface of the specimen and causes contamination problems. To solve this contamination issue without introducing any side-effects, the composition of standard lapping lubricant was focused and considered. Since the lapping lubricant comprises several additives such as surfactant, corrosion Inhibitors, wear inhibitors and viscosity index improvers, functional surfactants were considered to be added into the standard lubricant to solve the contamination problem during lapping process due to debris and particle redeposition. Surfactants with multiple characteristics have been normally employed in industrial as cleaner, detergent, emulsifier, dispersant, solubilizer, etc. [2]. The main

function of surfactant occurs form the existence hydrophobic and hydrophilic structure on the same molecule, that makes the molecule form aggregated structures, micelle at specific concentration, known as the critical micelle concentration [2]. There are several types of surfactants; non-ionic, anionic, cationic and amphoteric surfactants. The 3 different non-ionic surfactants were chosen in this work, ethoxylated alcohols (EAL), polyethoxylate alcohol (PEAL) and polyoxyethylene sorbitan monolaurate (PO). These 3 non-ionic surfactants have been widely used in many fields because of their good dispersion, emulsification and surface cleaning properties [3-6]. For cationic surfactants, cetyltrimethyl ammonium bromide (CTAB) and quaternary amines (QA) were chosen. These 2 cationic surfactants are commonly used for detergent boosting, corrosion inhibition, anti-static ingredients and emulsification [7]. For amphoteric surfactant, alkyl ethoxylated amine oxide (AAO) was selected which its properties are detergent and oxidation resistance [8].

In this work, functional surfactants were added into standard lapping lubricant to form their characteristics of the modified lubricants were investigated to fine the optimal condition to solve the metallic contact contamination during lapping process due to debris and particle re-deposition. The effects and mechanisms of surfactants in modified lubricants were investigated in different perspectives, including the anti-metal deposition, micelles formation above the critical micelle concentration and anticorrosion function.

1.2 Objectives

To study the effect of surfactants that were added into standard glycol-based lubricant can reduce and protect the slider surface from contaminant deposition and improve properties of modified lubricant at the same time.

1.3 Scope of this work

1. Verify surfactants that are used appropriately with lapping lubricant for slider lapping process.
2. Investigate the effects and mechanisms of surfactants in modified lapping lubricants.
3. Compare the efficiency of modified lubricants and provide the suitable lubricant for slider lapping process that can avoid the contamination problem during lapping process due to debris and particle re-deposition.

CHAPTER II

THEORY

2.1 Hard disk drive (HDD)

Data storage devises are a major technology, capacitate the digital universe due to the increasing volume of the data-storage devices.

Hard disk drive (HDD) is mainly used in the purpose of storage huge data information such as social network applications, internet services, mobile devices and massive data analytics. This means that the component parts inside HDD (head and disk) have to be developed to increase the larger data capacity. Figure 2.1 illustrates a hard disk drive with the important components parts [9].

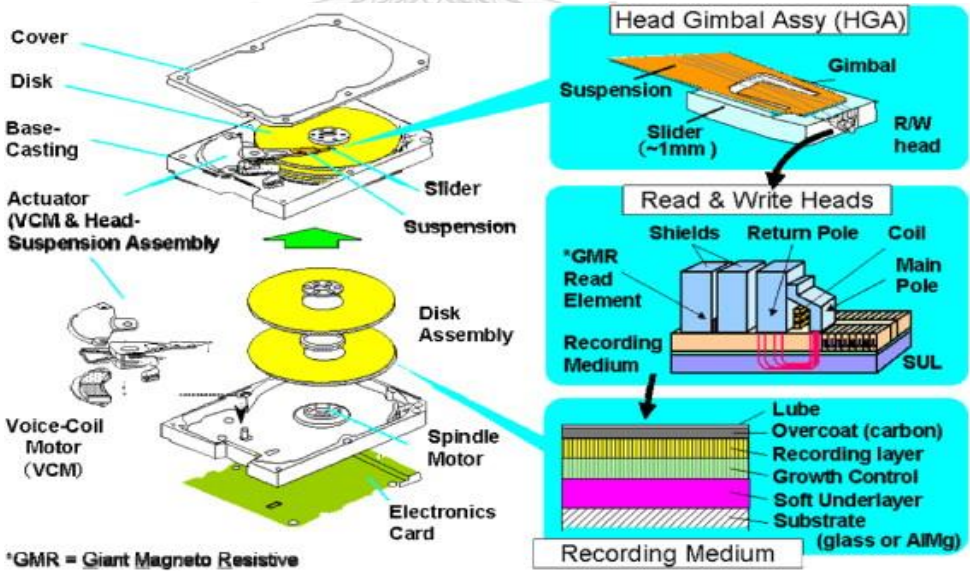

Figure 2.1 The structure and components in a hard disk drive [10]

The suspensions, which it has magnetic heads, were moved back and forth on the magnetic disk surfaces by the actuator motor. The head use magnetic fields to write/read data on the magnetic disk by using magnetic read-back sensors. The nanotechnology is used in the reading sensors, such as tunneling magneto-resistive heads. The disk is rotated by the spindle motor, underneath the head, which slider is attached on move along the disk surface. Moving of slider on the disk surface is a reading/writing data process. The surface of slider consists of many thin film layers (thin cushions) and the thickness of cushions is in the range of nanoscale. While slider fly on the spinning disk, it will create the air gap which is called “air bearing surface or ABS”. ABS support the slider close to but not touching the disk surface during reading and writing data. The circuit on the board of electronics HDD runs data into signals which are written on HDD or get the electronic signals from the reading sensors and shows it into digital data for the device using the hard disk drive [11, 12].

The performance of modern magnetic recording head (slider) is improved continuously, to increase the recording density up to the demand. The surface morphology of the slider consisting of many layers of thin film material such as Al_2O_3-TiC (AlTiC) for substate, cobalt-iron (CoFe) for writer and copper for reader, and nickel-iron (NiFe) of shield. Apart from the several types of materials, they are various physical properties. For instant, the hardened of AlTiC is much larger than NiFe and CoFe alloys [13]. The diagram of alloy multilayers of slider is shown in Figure 2.2.

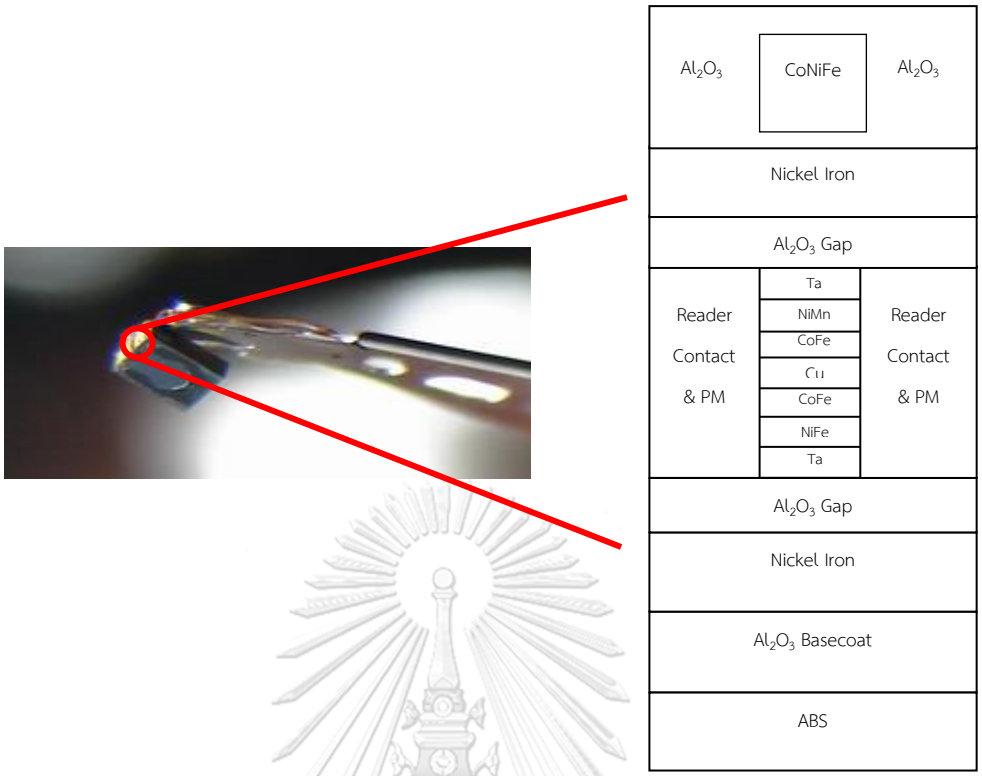

Figure 2.2 The diagram of alloy multi-layers of slider [13]

2.2 Slider lapping Process

The slider fabrication processes comprise of many procedures, as illustrated in Figure 2.3. First, each wafer that contained multilayers of alloy was loaded and ground wafer backside to decrease from initial wafer thickness to desire slider length. After that, the wafer was cut into individual row bars from wafer sectioning. The row bars were lapped on the back side to the specific thickness with stress management. Later, row bars were annealed at high temperature to reduce stress, which created during wafer sectioning and grinding processes. Next, the row bars were boned with wire on adhesive row tool and their thickness were rapidly decreased by removing material surface using lubricant and diamond slurry for rough lapping process. The final lapping process was used to control the surface roughness and morphology by using the standard glycol-based lubricant to controlling corrosion, workpiece surface finishing,

and material removal rate [14]. Last, all row bars were deboned and led to cleaning room for the next process.

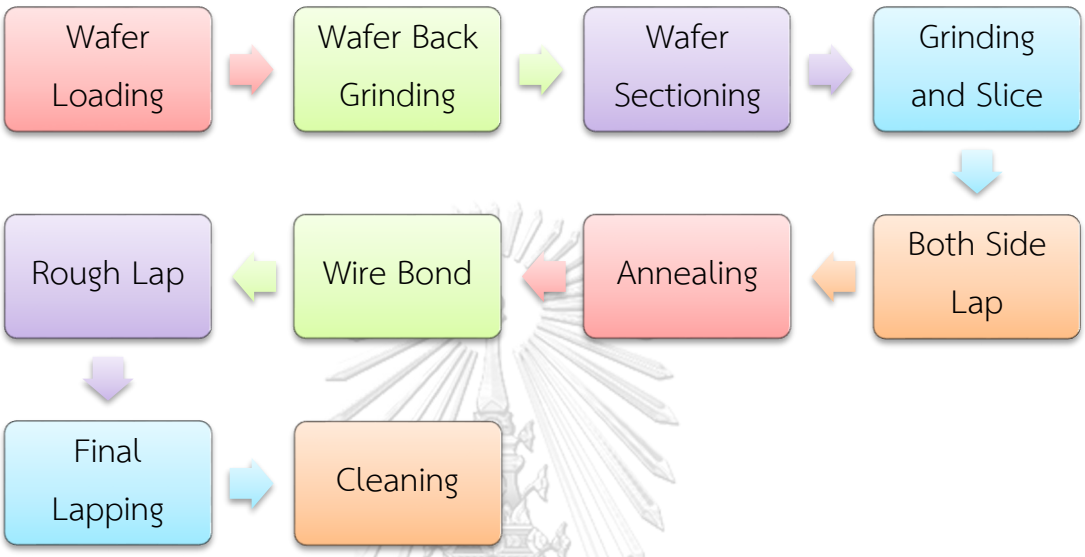

Figure 2.3 The slider fabrication process [14]

In the crucial final lapping process, there are many significant factors that affect the lapping performance and surface finishing, such as lapping plate, size of abrasive grains and lubricant. The based material of the lapping plate is Bismuth-Tin alloy with diamond abrasive grains imbedded on the surface. The lapping machine with the lapping plate is shown in Figure 2.4.

Figure 2.4 The lapping machine in the final lapping process [14]

2.3 Lubricants

The major functions of lubricants not only reduce the friction and wear, but also transfer heat, eliminate contaminant suspension, and protect corrosion between the surface of the materials [15]. There are various kinds of lubricant such as oil-in-oil emulsions (applied in metalworking), oil-in-water emulsions (used in water-miscible cutting fluids), water-based solutions (applied in chip-forming metalworking operations), water-in-oil emulsions (as in metal-forming), greases and solid lubricants [16].

Generally, Lubricants consist of based lube 70-95% and additives 5-30%, depends on the application. However, the based lubricant can be divided into 3 groups by their based lube as: petroleum-based, synthetic-based and environmental-based lubricants [17]. Moreover, the additives are the chemical compounds that were added into based-lubricant. Additives can create functional effects in lubricant in order to adjustment the performance of lubricant. The types of additive are diverse and shown in Table 2.1 [17].

Table 2.1 Major additive classes in lubricant [17]

Additive	Typical chemical	Objective
Anti-wear	Less reactive sulfur and phosphorous compounds	To reduce wear form wear-resistant reaction
Antioxidant	Amines and phenolics	To prevent the oil lubricants from oxidation
Detergent	Sulfonates, phenates	To collet contaminant suspension in motor oil
Dispersant	Succinate esters, Succinimides,	To reserve the contami-nant in suspension
Friction modifier	Esters and Long-chain fatty acids	To form thin films on the surfaces for easily shearing
Extreme pressure (EP)	More reactive sulfur compounds	To protect scraping by chemical reaction and providing protection
Viscosity index (VI)	Polyalkyl methacrylates, olefin copolymers,	To improve the VI to provide higher value
Multifunctional	Zinc dithiophosphates	To functions as anti-wear and antioxidant; invariably

2.4 Surfactant

Surface active substances or surfactants are a large number group of cleaning applications. Surfactants paly important role as detergents, wetting agents, emulsifiers, foaming agents, and dispersants. Most surfactants can generate self-assembled molecular clusters that was called micelles in a solution (water or oil phase), then the micelle adsorb to the interface between a solution and a different phase (gases/solids) [18].

2.4.1 Structure of surfactants

The structure of surfactant molecules comprises at least two parts which are the hydrophilic part and the hydrophobic part. The hydrophilic part is soluble in water and the hydrophobic part is insoluble. Moreover, the hydrophilic part is often referred as the polar head group and the hydrophobic part as the non-polar tail. The hydrophobic group is normally a hydrocarbon chain and the majority of these are linear for biodegradability demands. The structure is shown in Figure 2.5.

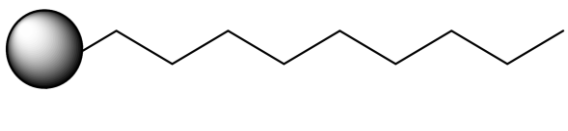

Hydrophilic head (Polar) Hydrophobic tail (Non-polar)

Figure 2.5 Structure of surfactants

2.4.2 Types of surfactant

These categories of surfactant are determined following to the type of ion that is soluble in water. Surfactant which can dissolve in solution and provide the negatively charged is called anionic surfactants. While cationic surfactants offer positively charged. Some surfactant has only tendency of electrical heads, not a full charge that is a nonionic surfactant. Another surfactants, the polar group can convert from negative to positive charged depending on the pH of solution.

Here are examples of four major classes of surfactants which applied in industry. These are: Amphoteric

- **Anionic surfactants**

Anionic surfactants are dissolved and their molecules isolated into anion in solution. They are the widely consumed surfactants that include alkylbenzene lauryl sulfate (foaming agent), sulfonates (detergents), lignosulfonates (dispersants), and di-alkyl sulfosuccinate (wetting agent) as seen in Figure 2.6. Anionic surfactants are employed around 50 % of the world manufacture [19].

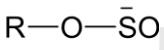

Alkyl sulfonate

(Used in shampoo)

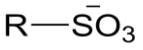

Alkyl sulfonate

(Used in cosmetic)

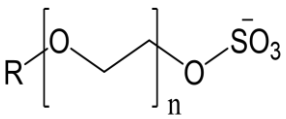

Alkyl ether sulfate

(Used in shampoo,

liquid soap)

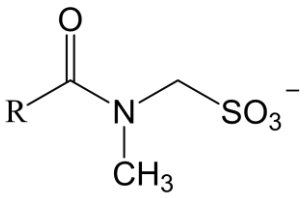

N-Alkyl-N-methy taurate

(Used in toiletry product)

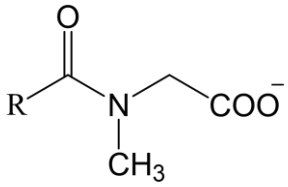

Alcylcarcosinate

(Used in toothpastes, care product)

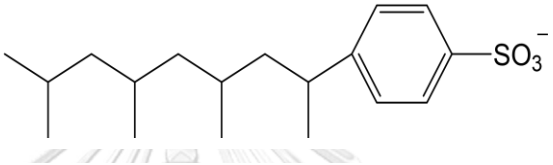

Alkyl benzene sulfonate

(Used in textiles, shampoo)

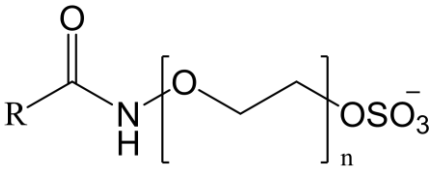

Alkylaminde ether sulfate

(Used in care product)

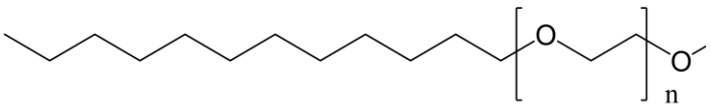

Ether carboxylate

(Used in cosmetics)

Figure 2.6 Anionic surfactant surfactants [20]

❖ **Cationic surfactants**

Cationic surfactants are contained a positively charged head, for example, a quaternary ammonium with alkyl chain group and fatty amine salts. The most advantage of cationic surfactants were found as **a** bactericides product for anti-microbials or anti-fungals. They are not good at foaming agents or detergent but their positive charge can adsorb on negatively surface, as the solid metal. Then, they can act as corrosion inhibitors, solid particale dispersant as well as floatation collector. The typical of cationic surfactant is as shown in Figure 2.7.

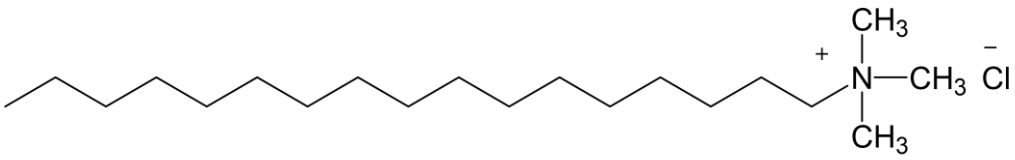

Alkyl quaternary ammonium salts

(Used in fabric softeners)

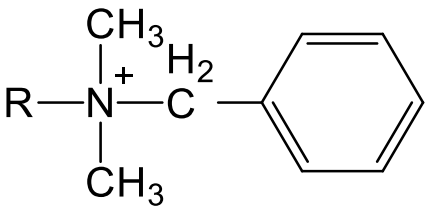

Alkylbenzydimethylammonium

(Used in cosmetic)

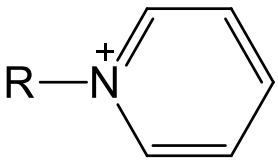

Alkylpyridinium

(Used in cosmetic, hair treatment, mouthwash)

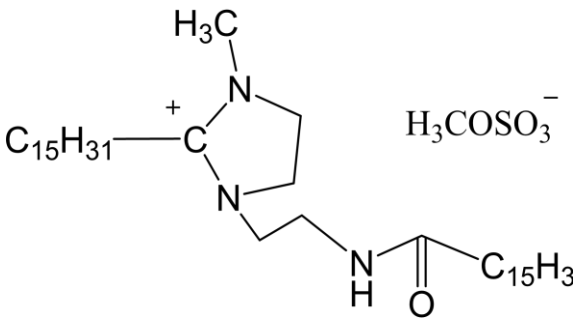

Quaternary imidazolium compounds

(Used in fabric softeners and antistatic agents.)

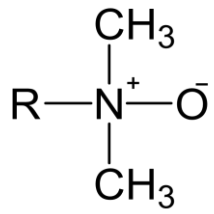

Alkyldimethylamine oxide

(Used in cosmetic, lotions)

Figure 2.7 Cationic surfactants [20]

❖ **Nonionic surfactants**

Nonionic surfactants are used in worldwide. Their hydrophilic part usually produces no charge in solution [20]. Since, their hydrophilic group (alcohol, phenol, ether, ester or amide) is not dissolve in solution, they hardly ionize in solution. A major proportion of these nonionic surfactants are made hydrophilic by a presence of polyethylene glycol chain that are called polyethoxylated nonionic. While some nonionic surfactant such as glucoside (sugar based) are shown lower toxicity, they are applied in many field [19]. The example of nonionic surfactant's structures is as shown in Figure 2.7.

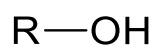

Alkyl Alcohols

(Used in cosmetic)

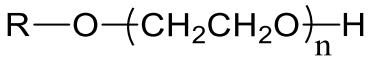

Ethoxylated alkyl Alcohols

(Used in low-foaming agents,

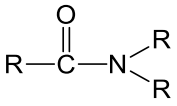

Alkyl amides

(Used in shampoo,

hair conditioner)

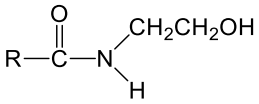

Alkyl monoethanolamide

(Used in cosmetic)

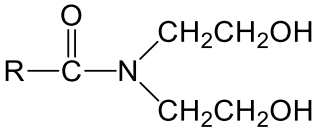

Alkyl diethanolamides

(Used in shampoos,

cosmetic)

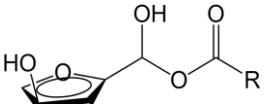

Sorbitan esters

(Used in cosmetic)

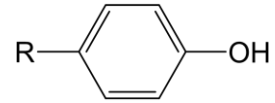

Alkylphenol

(Used in low-foaming

agents)

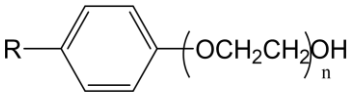

Ethoxylated alkylphenol

(Used in shampoo)

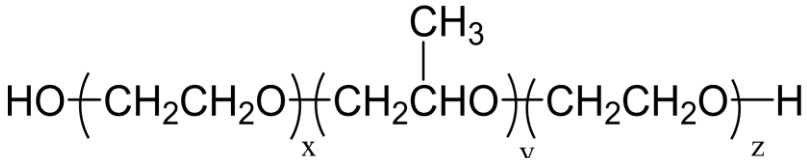

Ethylene Oxide/Propylene Oxide Copolymers

(POE/POP, used in cosmetic, detergents, emulsifiers

and antistatic agents.)

Figure 2.8 Nonionic surfactant surfactants [20]

❖ **Amphoteric /Zwitterionic surfactants**

Amphoteric or zwitterionic surfactants have both functional group cationic and anionic that mostly depend on pH. When solution is acidity, surfactants paly as cationic. Another pH, basicity solution allow surfactant to anionic. They are applied as hair and fabrication conditioner, antistatic additive, detergent and foaming agent [19-20]. Some of amphoteric surfactants are shown in Figure 2.9.

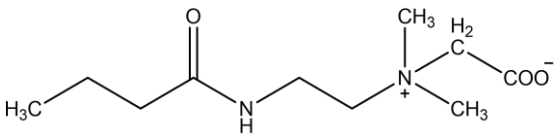

Alkylamidopropylbetaine

(Used in cosmetic, toiletry products, shampoo)

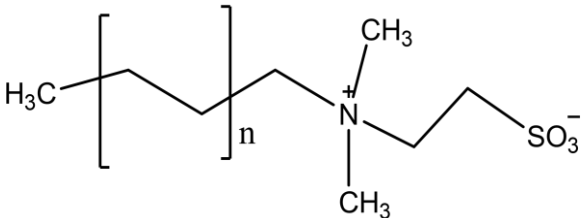

Alkyldimethylsulfobetain

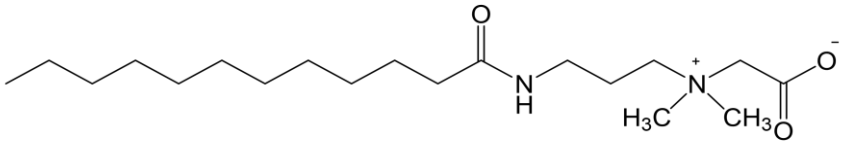

Cocamidopropyl betaine

(Used in facial cleanser, hair conditioner)

Figure 2.9 Amphoteric (zwitterionic) surfactants [20]

2.5 Micelles

2.5.1 Micellization

One of the most significant characteristics of surfactants is that when they reach a certain concentration, the surfactant molecules associate and create a micelle (in most cases a spherical micelle), a self-assembled molecular cluster. The critical micelle concentration (CMC) is defined as the concentration where surfactants form micelles.

The key to forming micelles in aqueous solutions is the interaction between hydrophilic and hydrophobic, which this interaction will increase entropy in the water molecules that interact with these surfactant molecules.

The adding surfactants into water, the water molecules surround the hydrophobic groups create an iceberg structure, causing the entropy of the water molecules to decrease. As the concentration increases and the number of surfactant molecules increases, the hydrophobic groups encounter each other and start to associate, causing the iceberg structure to collapse and release free water. When free water is released, the entropy of water molecules increases (the decrease of entropy caused by the association of hydrocarbons is significantly smaller than the entropy increases of water), and this energy triggers micellization [21].

A surfactant shows different properties in aqueous solutions when it exists as single molecules and when they reach their micellization concentration, so the CMC can be determined by observing the solution's conductivity, surface tension, osmotic pressure and etc.

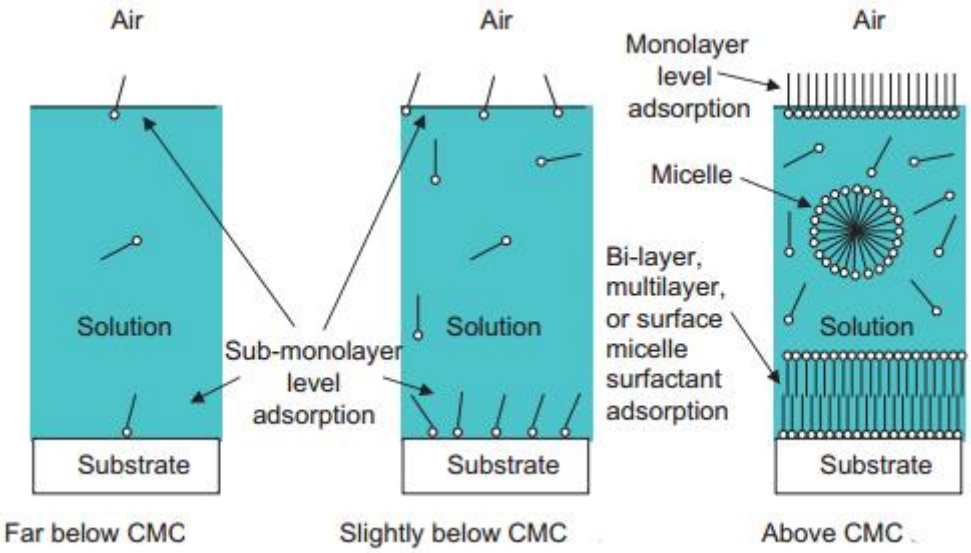

Figure 2.10 Schematic illustrating the surfactant aggregation and adsorption as a function of relative surfactant concentration of relative surfactant concentration [21]

Above the CMC value, the monomers aggregate to form micelles. Such a self-organization (Figure 2.10) is a reversible process and it depends on the thermodynamics of the solution. Under low concentrations, the block copolymers occupy as monomers and above CMC the entropy of the system decreases, owing to the molecular organization of the solvent. Then, dehydration of the hydrophobic tails tends to block copolymers aggregating to form micelles, an increase in entropy occurs, favored by hydrophobic interactions between block copolymers. Additionally, the formation of Van der Waals bonds allows the hydrophobic polymers to join and to form the micelle core. The result of hydrophilic shell regenerate hydrogen bond networks with the surrounding water [21].

The value of CMC is an important parameter in many industrial applications involving adsorption of surfactant molecules at interfaces, such as foams, froths, emulsions, suspensions, and surface coatings. It is probably the simplest means of characterizing the colloid and surface behavior of a surfactant solute, whereas determines its industrial advantage.

2.5.2 CMC measurement

The CMC can be determined from the breaking or inflection point in the plot of a physical property of the solution as a function of surfactant concentration. Clear breaks of almost every measurable physical property are shown in Figure 2.11[22].

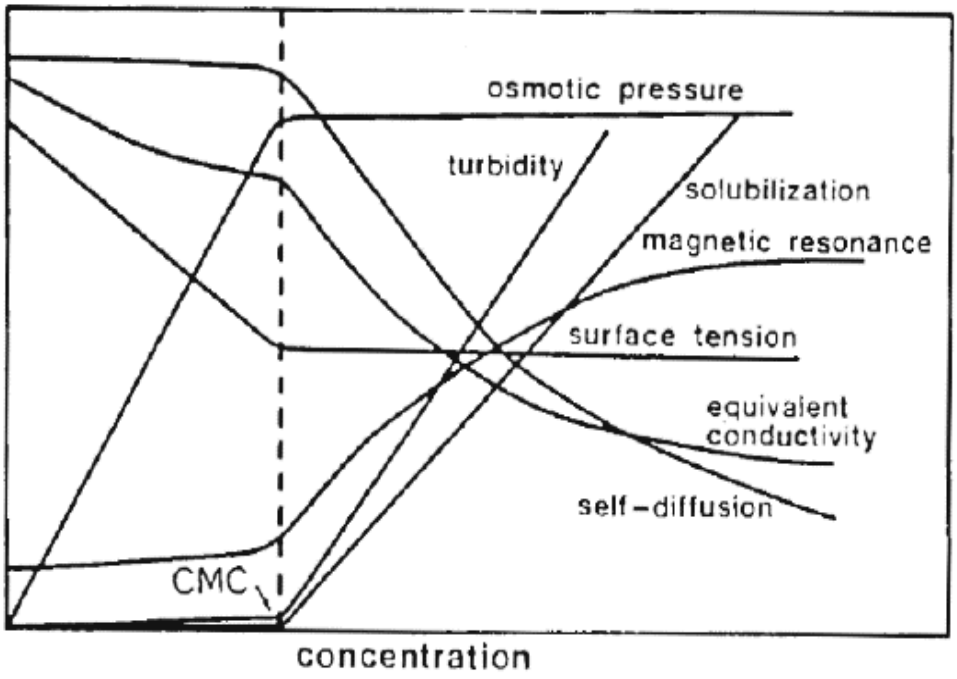

Figure 2.11 Change in concentration dependence of a wide range of physico- chemical quantities around the critical micelle concentration [22]

2.5.3 Steady-state fluorescence intensity

The CMC can be measured by Fluorescence spectroscopy [23]. Pyrene has been used for more than a half decade as fluorescent probe par excellence for microheterogeneous systems such as micelles [24]. The fluorescence intensity of pyrene in the solvent polarity is widely used for the determination of the CMC of micellization. The photophysical behavior of pyrene in microheterogeneous systems has been the object of many detailed studies and reviews. The fluorescence spectrum of pyrene shows characteristic vibronic bands around 370–400 nm. The diffusion-controlled formation of excimers quenches the pyrene fluorescence emission. The

ratio of the fluorescence intensities of the first and third vibronic bands of pyrene (I_1/I_3 ratio) was observed. The break point in the plot of I_1/I_3 ratio vs calixarene concentration furnishes the CMC value. Figure 2.12 describe the determination of the CMC of adenine 20 deoxynucleotide calixarene by pyrene fluorescence spectroscopy method [25].

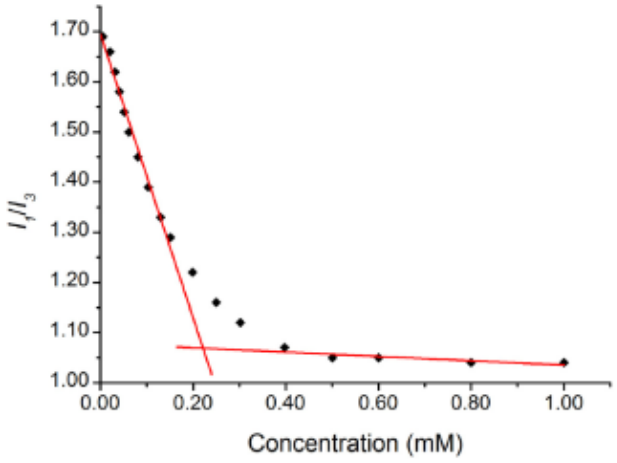

Figure 2.12 Determination of CMC of adenine 20-deoxynucleotide calixarene by using fluorescence spectroscopy. The plot intensity of I_1/I_3 ratio vs adenine 20-deoxynucleotide calixarene concentration; [pyrene] 0.5×10^{-6}M, excitation 333 nm [25].

2.6 Characterization

2.6.1 Scanning Electron Microscopy (SEM)

The scanning electron microscope (SEM) is used for the multipurpose and the schematic of SEM is as shown in Figure 2.13. It can be identified the microstructure morphology and chemical composition characterizations [26]. Electrons are produced at the electron gun filament and passed through electron lenses to create a focused beam of electrons which emitted the surface of the specimen. Position of the electron beam on the sample is controlled by scan coils situated above the objective lens. The beam is allowed to be scan over the sample's surface by these coil [27-30]. Presently, SEM usually assigned with an EDX analysis system to perform compositional analysis

on samples. EDX analysis is beneficial in identifying element and composition, as well as calculating their relative concentrations on the surface [31].

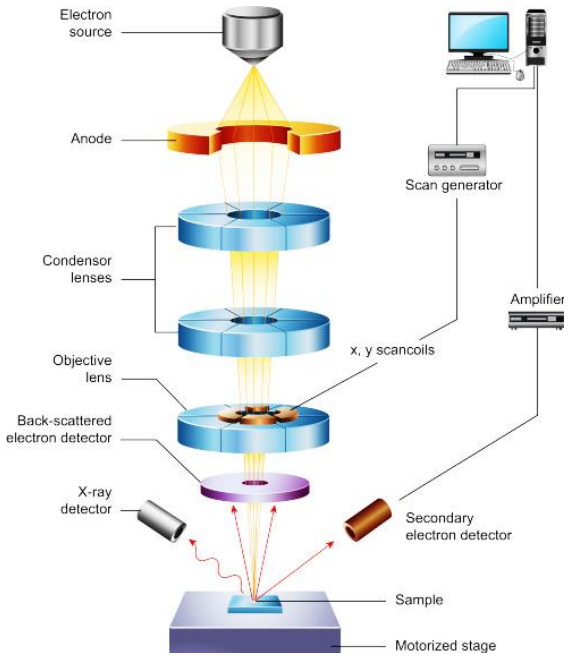

Figure 2.13 Structure of SEM [26]

2.6.2 Fluorescence microscopy

The fluorescence microscope certain material emits energy detectable as visible light when irradiated with a specific wavelength of the light (see Figure 2.14). The sample can be fluorescing in its natural form like chlorophyll and some minerals or retained with fluorescing chemicals. Light of the excitation wavelength illuminates the specimen through the objective lens. The fluorescence emitted by the specimen is focused to the detector by the same objective that is used for the excitation. Since most of the excitation light is transmitted through the specimen, only reflected excitatory light reaches the sample together with the emitted light and the epifluorescence method therefore gives a high signal-to-noise ratio. The dichroic beam

splitter acts as a wavelength specific filter, transmitting fluoresced light through to the eyepiece or detector, but reflecting any remaining excitation light back towards the source [32-34].

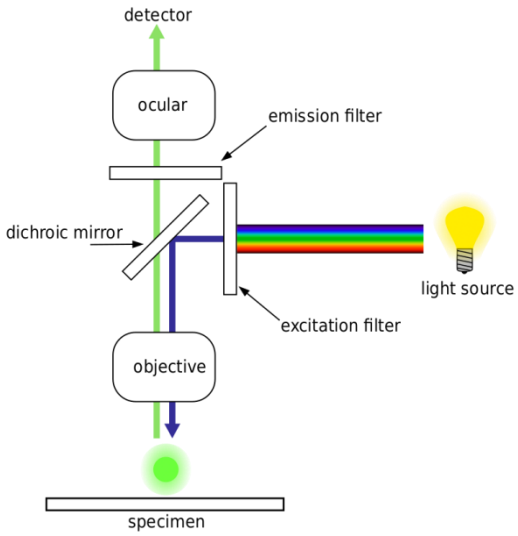

Figure 2.14 Schematic of a fluorescence microscope [35]

2.6.3 Quasi-static test (QST)

Quasi-static Test or QST is a measurement system to analyze the electrical performance of a slider. QST is used as guidance to screen out sliders with poor electrical performance of magnetic head. MRR and Amplitude are important parameters that obtained from the QST. MRR or Magneto Resistive Resistance is a measurement of resistance across the shield of MR element. Low MRR indicate that there is some bridging or smearing of the shield causing high electrical conductivity. In this work, the percentage of the change in MRR (%ΔMRR) is calculated. The schematic measurement diagram of QST is shown in Figure 2.15.

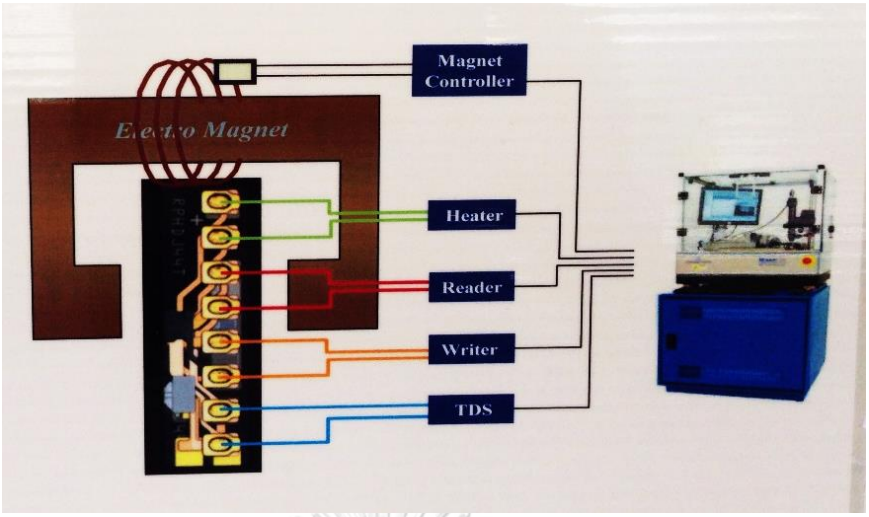

Figure 2.15 Schematic measurement diagram of QST [14]

2.6.4 Corrosion

Corrosion is another kind of redox reaction. Corrosion occurs from the destructive attack of metals by chemical or electrochemical reaction with the environment. The metal formed oxidation and occur at anode, while protons receive electrons as reduction for cathode [36, 37]. Polarization is a common method used to explain the corrosion behavior of metal or material and its environment using kinetic principles. In this measurement, the potentiodynamic polarization curve is obtained. Corrosion current density (i_{corr}) is a corrosion current divided by corrosion surface area. Corrosion current density and corrosion potential (E_{corr}) are estimated by the method of linear-polarization of Tafel extrapolation [38-40]. Corrosion rate is a significant parameter for measuring the effect of lubricant on the corrosion of metals, which can be calculated from Equation 2.1 and 2.2 [38-40].

$$CR = \frac{0.13 \text{ x } i_{corr} \text{ x EW}}{p}. \quad 2.1$$

$$EW = \frac{1}{\sum \frac{n_i f_i}{A_i}} \quad 2.2$$

When, CR = Corrosion rate (mm/year)

i_{corr} = Current density (μA/cm^2)

EW = equivalent weight of metal (g/equivalent)

p = density of metal (g/cm^3)

2.6.5 Tribology

Tribology is the science that focused on friction, wear and lubrication. It studies the interaction of moving during the contacts of two material surfaces. Tribology solutions are applied in automotive industry, sports, food, health and biomedicals, renewable energy and other various fields. The importance of tribology rises due to the fact that frictional and wear losses consume energy, which otherwise could be saved [41].

Friction is a force that resists the motion. Friction force is occurred at the interface between the materials. The surface contact area of the object has normal force (F_n). When two objects are in contact motion, the friction force (F_S) will be occurred the frictional force (F_S) depends on the applied normal force (F_n) and is described by Equation 2.3. Where μ is coefficient of friction (COF) [41-43] and Illustration of basic frictional forces is shown in Figure 2.16.

$$F_s = \mu \times F_n \quad (2.3)$$

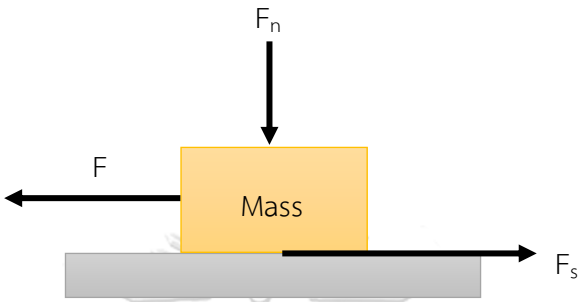

Figure 2.16 Illustration for applied the basic frictional forces [41, 43]

One of the simple ways for measuring the static COF is ball-on-disk tribometer. Tribometer is the device used to analyze and characterize tribological parameters (see Figure 2.17). The most common measurement is the measurement of COF. During the post processing stage other quantities can be measured, such as wear volume, surface roughness evolution, tribofilm thickness, etc. There are many types of configuration of tribometer devices such as a pin-on-flat, pin-on- disk, ball-on-disk or sphere-on-ring. For the ball-on-disk tribometer, the sample disk is rotated at a selected speed. The normal force will be applied through the ball. The friction track formed by the ball on the sample. The COF is determined during the test by measuring the signal from force sensors [44].

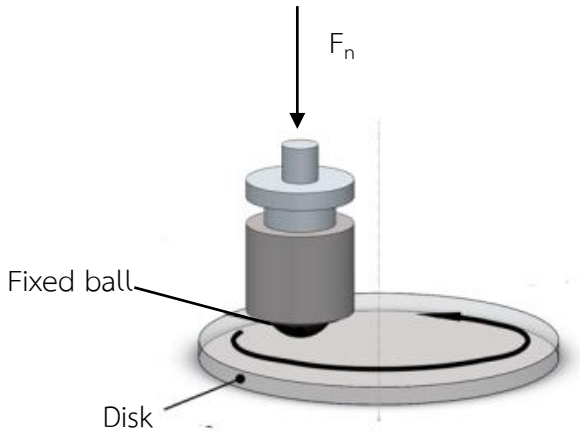

Figure 2.17 Schematic diagram of the ball-on-disc point contact device [45].

2.7 Literature reviews

The studied of attached Bi have been done by many researchers. The bismuth in pharmaceutical products was determined by using methyltriphenylphosphonium bromide as a molecular probe based on the resonance light scattering (RLS) technique that were studied by Fengling C. and et al. [46] in 2007. To form $[BiI4]^-$, bismuth reacted with a large excess of I^-. Then, it reacted with methyltriphenylphosphonium bromide (MTPB) in order to form an ion-association compound. This led to a significant enhancement of RLS intensity and the appearance of the corresponding RLS spectral characteristics.The concentration of Bi (III) in the range of 0.001–1.50 μg/ml affected directly to the enhanced RLS intensity with the detection limit of 0.98 ng/ml. The optimum conditions and the influencing factors were investigated and it was found that the characteristics of RLS spectra were high selectivity. Moreover, this method was applied to determine concentration of Bi (III) in pharmaceutical products.

In 2011, Didi M. and et al. [47] studied two-aqueous phase extraction of bismuth (III) as a solute from its aqueous solutions. It was investigated by using polyethoxylated alcohols (C12E10, C13E10). The structure showed in Figure 2.18. They act as a biodegradable non-ionic surfactant by cloud point extraction (CPE) that can be applied for the extractive concentration, separation and purification of metal ions, metal chelates, biomaterials and organic compounds.

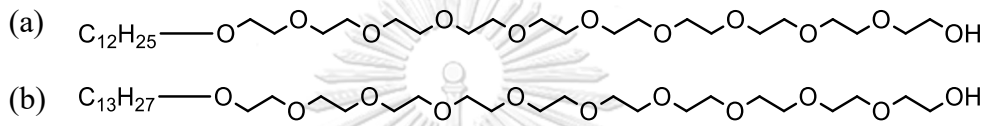

Figure 2.18 a) C13E10 is decaethylene glycol monotridecyl ether. b) C12E10 is decaethylene glycol monododecyl ether.

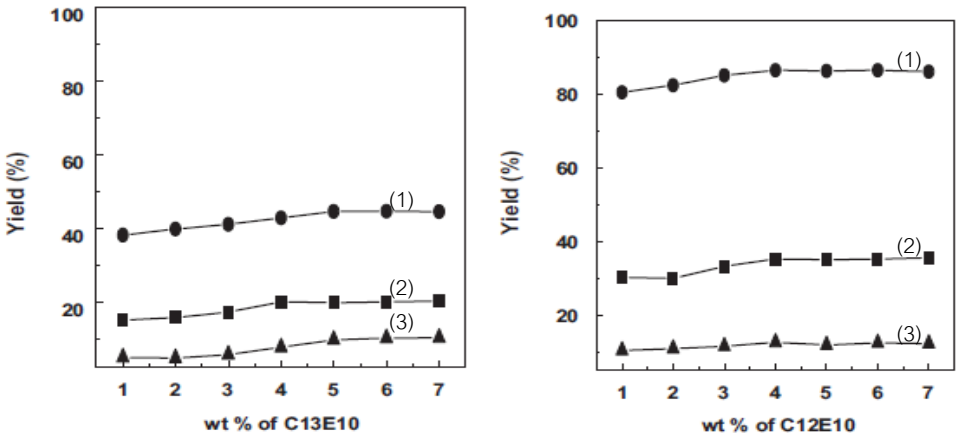

Figure 2.19 The effect of non-ionic surfactant on the extraction yield in H_2O/surfactant/$Bi3^+$: (1) C13E10 at 60 °C for 5% of NaCl, (2) C13E10 at 69 °C and C12E10 at 97 °C for 0% of NaCl, (3) C12E10 at 70 °C for 10% of NaCl

The results of the experiments were shown in Figure 2.19 and carried out and the percentages of extraction vary from 34% to 86%. The optimal condition is the concentration of the surfactant C12E10 at about 1%wt, a 5 %wt of NaCl, a temperature below than 5°C to the cloud point of surfactant used (T=70°C) and times of decantation at 24 hours.

Then, emulsion liquid membrane (ELM) technique from nitrate medium based on the optimization of experimental parameters, that were used to extract Bi (III), were studied by Mokhtari B. and Pourabdollah K. in 2015 [48]. This technic used di(2-ethylhexyl) phosphoric acid (D2EHPA) as carrier and isooctylphenoxy-polyethoxyethanol (Triton X-100) as biodegradable surfactant. The results showed in Figure 2.20. Bi (III) was extracted with D2EHPA that fixed on an Amberlite XAD-1180 solid support. The addition of saoking aqueous volume declined the sorption of Bi (III). Moreover, the antagonistic effect on the cation sorption was observed by adding sodium chloride. Measurement of trace amounts of Bi (III) had expanded by cloud point extraction (CPE) followed by flame atomic absorption spectrometry. The Bi (III) ions were extracted by 100% in this study. The liquid membrane was becomed from 1% D2EHPA with Triton X-100 (0.5%) in the n-pentanol bulk membrane. The emulsion was operated with sulfuric acid solution (0.5 mol·L^{-1}) under 1800 r·min^{-1} of stirring for 20 min. The best extraction of Bi (III) ions from nitrate medium was provide by using 350 mg·L^{-1} feed concentration and 30 minutes of equilibrium time under 210 r·min^{-1} of stirring.

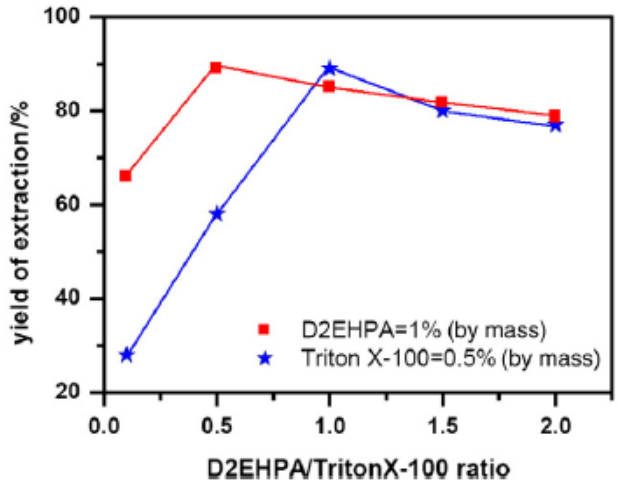

Figure 2.20 Effect of ratio D2EHPA/Triton X-100 on the extraction of Bi (III). Stripping solution: 4.5 ml of H2SO4 (0.5 mol·L^{-1}); stirring: 210 r·min^{-1}; [$Bi3^{+}$] = 500 mg·L^{-1}.

The affection of the ratio D2EHPA/Triton X-100 on Bi (III) extraction was studied (see Figure 2.14). The concentration of extractant was fixed and the concentration of surfactant was varied. The liquid membrane was upon dichloromethane as diluent. Figure displayed that the extraction yields of Bi (III) enhanced with the ratio D2EHPA/Triton X-100 in both cases, reaching about 80%.

In 2015 Ponzoni C. and et al.[49] studied electrostatic stabilization of bismuth ferrite $BiFeO_3$ (BFO, see Figure 2.21). To investigate forming homogeneous films through electrophoretic deposition technique, they first did the experiment in aqueous medium and using sodium polyacrylate (Na-PAA) as suspending agent which these solutions contain single phase micronized particles suspended. The dispersion efficiency was calculated in terms of the zeta potential trend as a function of pH and sediment percentage. It employed a fast and simple spectrophotometric method. All the tests were conducted using three suspending agents characterized by the same polyacrylate functional group (-COONa) but with different molecular weights (Na-PAA Mw 2,100, 5,100, and 20,000). They studied the effect of of BFO particles concentration

(%wt) on suspending agent concentration (%wt), suspending agent molecular weight and sonication time. It was found that for all the experiments carried out the electrostatic stabilization of the BFO micronized particles in aqueous medium. It is achieved in high basic pH range (8.5-9 or 9-11) to depend on the molecular weight of the polyacrylate additive.

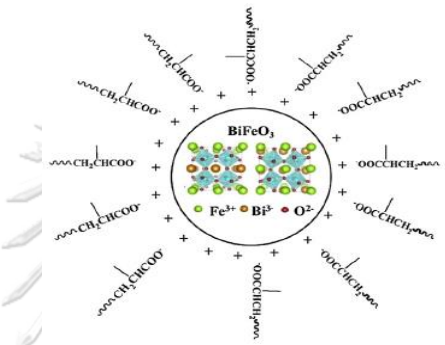

Figure 2.21 Structure of bismuth ferrite $BiFeO_3$ suspensions in aqueous medium

According to Shubha H.N. and et al. [50] work, they studied another surfactant which is cetyl-trimethyl ammonium bromide (CTAB). They focused to empower the corrosion resistance property by self-assembled monolayer (SAM) on mild steel. There are two parameters (pH and time) that were optimized. The results form SAM with the condition of 1 mM solution of CTAB at pH 2.5 for 2 hours demonstrated a regimented monolayer. Polarization and electrochemical impedance spectroscopic (EIS) were studied for an important enhancement in the corrosion resistance property on protected steel within conditi9on of both 1 M HCl and 3.5% NaCl solution. The surface from CTAB experiment reduced the corrosion rate about 4 times in 1 M HCl and 1.5 times in 3.5% NaCl media as compared to bare steel respectively. Electron micrographs from SEM confirmed a small amount of CTAB can protect surface.

CHAPTER III

THE EXPERIMENTS

3.1 Materials

The slider bars consist of many thin films of materials, grown on Al_3O_2 (AlTiC) and AlTiC with iridium-manganese (IrMn) were supplied by Western Digital (Thailand) Co., Ltd.

3.2 Chemicals

1. Glycol-based lubricant (Innovative Organics Company)
2. Ethoxylated amine oxide, EAO (Saint Gobain Ceramic Materials)
3. Ethoxylated alcohols, EAL, Tomadol 900 (Air Product industry co. ltd)
4. Decaethylene glycol monododecyl, PEAL (Sigma Aldrich)
5. Cetyltrimethyl ammonium bromide, CTAB (EMD chemical; Germany)
6. Alkylated amineoxide, AAO, Tomamine AO-14-2 (Air Product industry co. ltd)
7. Quaternary amines, QA, Tomamine Q-14-2, (Air Product industry co. ltd)
8. Polyoxyethylene-(20)-sorbitanmonostearate, Tween 20, PO (Chemipan Corporation Co., Ltd., Thailand)
9. Glacial acetic acid (Merck, 100%)
10. Potassium hydrogen phthalate, KHP (Merck, 99%)
11. Chlorobenzene (Merck, 99%)
12. Perchloric acid (Merck, 70-72%)
13. Pyrene (TCL, 99%)

3.3 Deposited contaminant analysis

3.3.1 Deposited contaminant characterization

The electroplating experiment was set up to duplicate an electrostatic deposition occurred during the lapping process. The Cu electrical plate (1x0.5 cm) and a piece of Bi/Sn lapping plate were used as cathode and anode, respectively. The sludge was the used standard glycol-based lubricant that contained many particles such as heavy metals, debris and dust. The sludge was directly collected from lapping process of sliders, in order to use as electrolyte as shown in Figure 3.1. To verify the black deposited contaminant on surface. The voltage was operated at 2 V for 5 hours and at 4 V for 2 hours, in electrodeposition process. Then, the Cu plate was annealed in oven 24 hours and analyzed the surface by using JEOL JSM-7610F field emission scanning electron microscopy (FESEM) and Oxford X-MaxN 20 energy-dispersive X-ray spectroscopy (EDS).

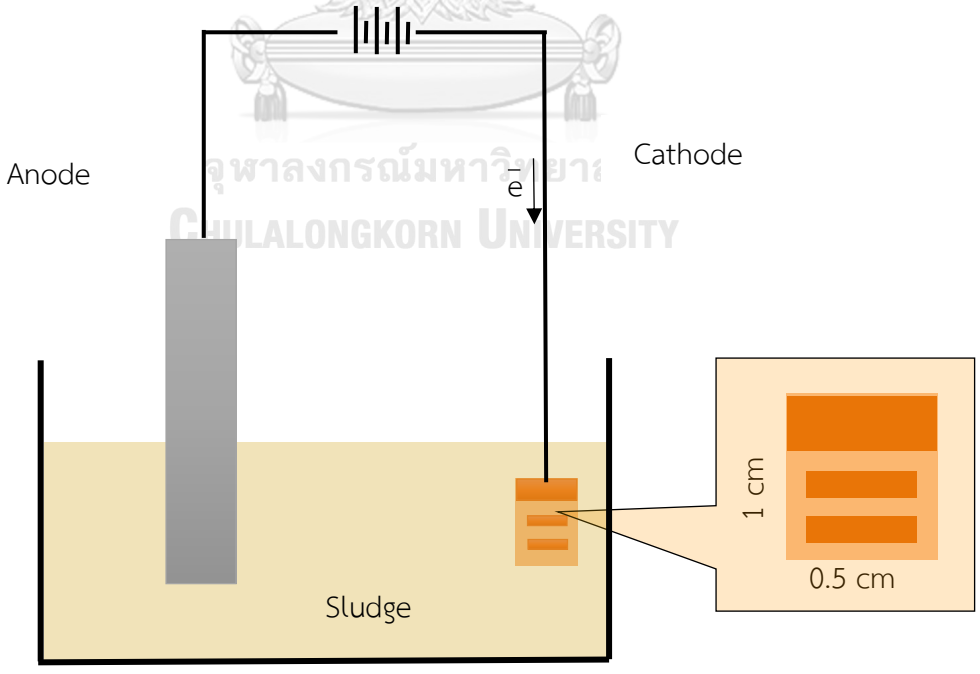

Figure 3.1 Schematic of deposited contaminant characterization

3.3.2 Surface deposition characterization

The surface of the specimens was studied by electroplated of the sludge mixed with various surfactants, as electrolyte, on the Cu test specimens (Figure 3.2). The surfactant concentration for each electrolyte was fixed at 1.0 %wt. Electrodepositing was carried out at voltage at 1.5 volts for 20 minutes. After that, the surface was investigated by using JSM-5410 LV scanning electron microscope (SEM), operated at 15.0 kV of an accelerating voltage.

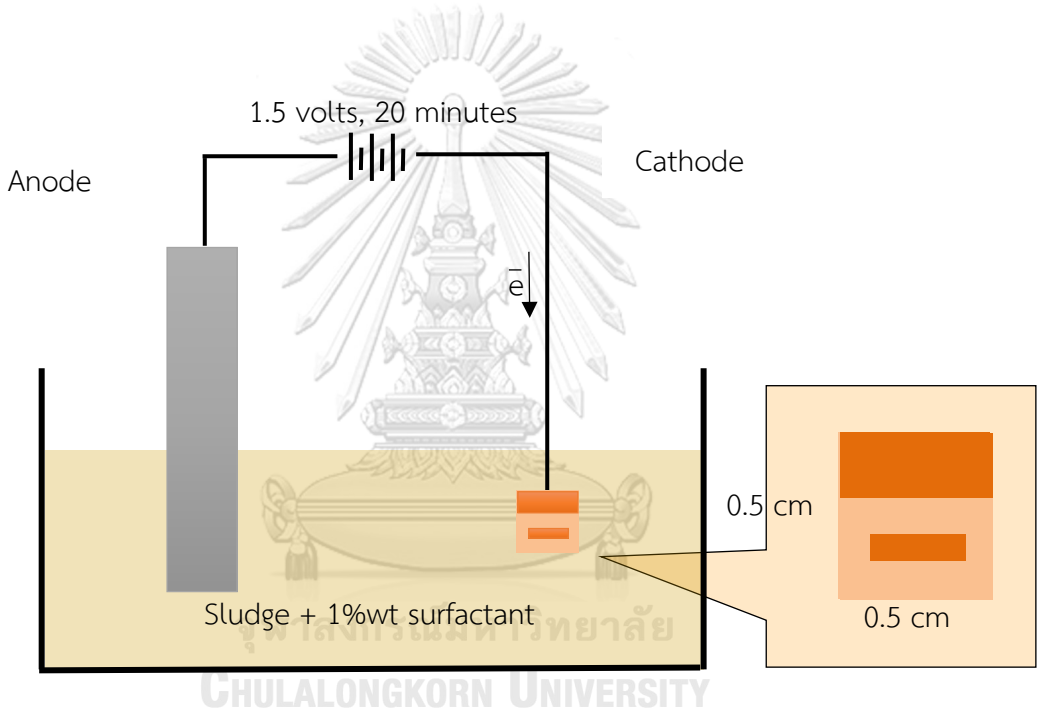

Figure 3.2 Schematic of surface characterization

3.4 Functional surfactant mechanism studies

The fluorescence studies were investigated, according to Prasun et al [51]. The characterizations were performed, using a Cary Eclipse, Algilent Technologies spectrophotometer. Stock solutions of pyrene ($1x10^{-3}$ M) were prepared in ethanol, and the last concentration of pyrene was fixed at $1x10^{-6}$ M for all experiments. The first vibronic band (I_1) and the third (I_3) vibronic band of the emission spectrum of pyrene were monitored at 375 and 392 nm, respectively. The excitation wavelength was set to 337 nm. The slit widths of excitation and emission were set at 5 nm. The different concentrations of surfactants- PEAL, QA and PO were added to the standard based-lubricant to obtain each modified lubricant. The stock of PEAL, QA and PO modified lubricant were prepared and diluted with ethylene glycol.

3.5 Preparation and characterization of modified lubricant

The different concentrations of PEAL, QA and PO surfactants (0%, 0.2%, 0.4%, 0.6%, 0.8% and 1.0%) were added into standard glycol-based lubricant to obtain 5 groups of lubricant for each additional surfactant. Ratio of surfactant and other chemicals of the modified lubricants are shown in the Table 3.1.

Table 3.1 Concentration of lubricant samples

lubricant	EG (%wt)	Water (%wt)	Surfactant (%wt)
Standard lubricant (SL)	93.126	6.882	0.0
PEAL-Modified lubricant	92.926	6.882	0.2
	92.726		0.4
	92.526		0.6
	99.326		0.8
	99.126		1.0
QA-Modified lubricant	92.926	6.882	0.2
	92.726		0.4
	92.526		0.6
	99.326		0.8
	99.126		1.0
PO-Modified lubricant	92.926	6.882	0.2
	92.726		0.4
	92.526		0.6
	99.326		0.8
	99.126		1.0

To characterization the basic properties of modified lubricants. The pH and conductivity values were measured by using the pH/conductivity meter (S470 SevenExellenceTM, Mettler Toledo). A 20 ml of each lubricant was used in each measurement. The measurement was repeated for three times of each modified lubricant. The total base number (TBN) was also measured following ASTM-D2896, using auto-titration method (DGi116-solvent glass pH electrodes, Titration Excellence T50, Mettler Toledo) to determine basicity values of the modified lubricants which can be shown in terms of the equivalent number of milligrams potassium hydroxide per gram (mg KOH/g).

3.6 Performance of lubricant

3.6.1 Quasi-static test (QST)

QST is a system to measure the change of magnetoresistive resistant (MRR) value of a slider. The MRR data was used to analyze the performance of our modified lubricants in this work. Sliders were measured before the lubricant soaking. Then, sliders were immersed in the modified lubricant, which standard based-lubricant were mixed with different surfactants (PEAL, QA and PO) with 5 different concentrations for each surfactant, as 0%, 0.2%, 0.4%, 0.6%, 0.8% and 1.0%, respectively. After soaking, the sliders were measured for the QST parameters again. The percent of MRR changes were analyzed and calculated to optimize the working concentration of the surfactants. The process of test QST are:

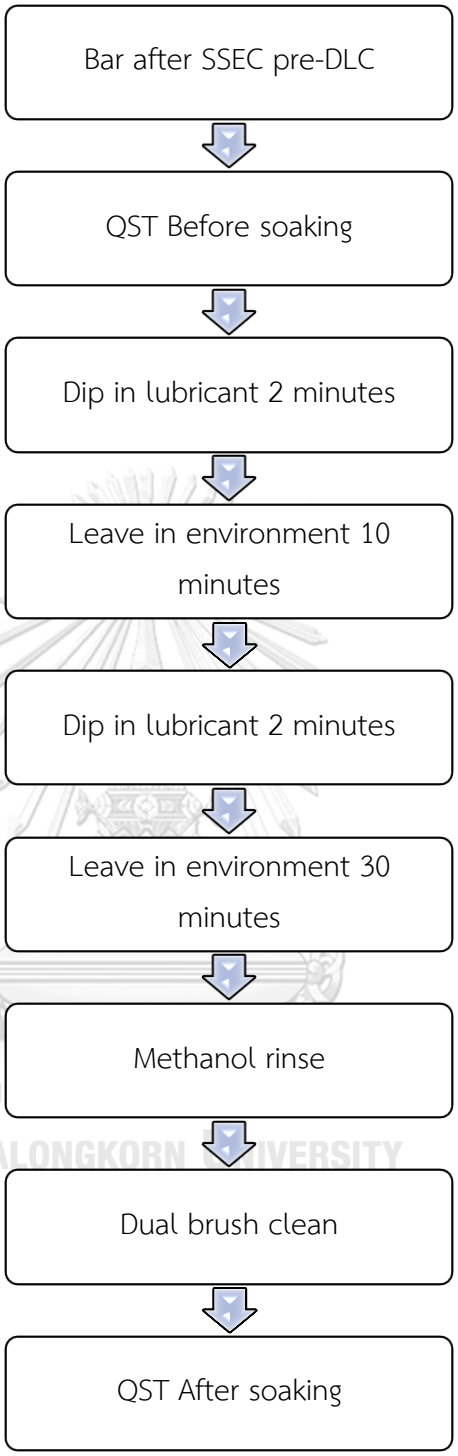

Figure 3.3 The process of test QST

3.6.2 Potentiostat polarization measurement

Potentiostat polarization measurement was applied to measure the corrosion potential (E_{corr}) and corrosion current (I_{corr}), to obtain the corrosion rate and corrosion behaviors of the modified lubricant on wafer that was coated with iridium-manganese (hot IrMn 79, Western Digital (Thailand) Co., Ltd.). The measurement was carried out by using Potentiostat (EG&G Model 273). A general three probes with a platinum counter-electrode and an Ag/AgCl as a reference probe were used. The specimen was cut into 2 cmx2 cm for using as working electrode. 1 %wt PEAL, 1 %wt QA and 0.2 %wt PO modified lubricants were used as electrolyte in this experiment. The potentiometer was performed at 300 sec OCP (open circuit potential) ,0.00122 step potential, 0.002 v/s scan rate, -1,0.6 V potential range by using Autolab 1.9.16, Nova 19 software that was shown in Figure 3.4.

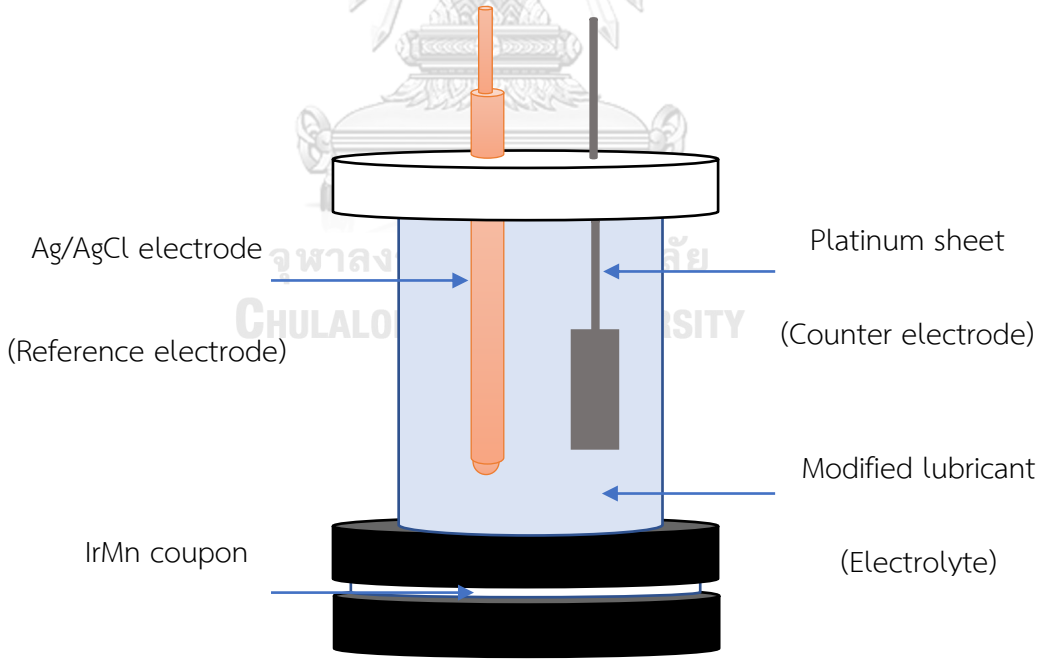

Figure 3.4 Illustration of flat cell potentiostat

3.6.3 Lapping test

The ASL 200 final lap machine is the device to polish/lap the sliders to desire roughness properties in slider fabrication. The 1 %wt PEAL, 1 %wt QA and 0.2 %wt PO modified lubricant were carried out with the process final lapping machine using actual Bi-Sn lapping plate at speed of lapping plate of 10 rpm. The lapping condition is the same as industrial work to reach target resistance. The lapping time and the surface finishing performance of modified lubricant were observed.

Figure 3.5 Physica MCR 301, Anton Paar rheometer [52]

3.6.4 Viscosity test

Rheometry describes measuring method that was used to determine rheology properties. Viscosity properties of modified lubricant were investigated by using Physica MCR 301, Anton Paar that was shown in Figure 3.5. The 1 %wt PEAL, 1 %wt QA and 0.2 %wt PO modified lubricant were performed. The experiment was operated at room temperature.

3.6.5 Tribology test

Tribological measurements of optimum modified lubricant were carried out on a micro-tribometer (UMT-2, CETR) (Figure 3.6) to observe Lubrication properties. The equipment was used ball-on-disk technique. A 6.35 mm stainless-steel ball was used to test on AlTiC disk. The applied loads were 0.5 N and the sliding speed 3600 mm/min. The experiments were realized at room temperature. The 15 g of sample was used for each test, which was gently spread to completely cover the AlTiC plate surface.

Figure 3.6 UMT-2, CETR [52]

Chapter IV

RESULTS AND DISCUSSIONS

As mention in the motivations of this thesis, there was a contamination deposition found during the lapping process in slider fabrication. The gold (Au) electrical contacts on slider were covered by the black contaminant layer, as shown in Figure 4.1. They were subjected for contaminant analysis to verify their surface properties. The contamination characterizations were carried out using electroplating for substitution electrostatic force during lapping process and the copper (Cu) electrical contacts were used instead of Au contacts for this study. The electrodeposited Cu plates were characterized, using SEM-EDS.

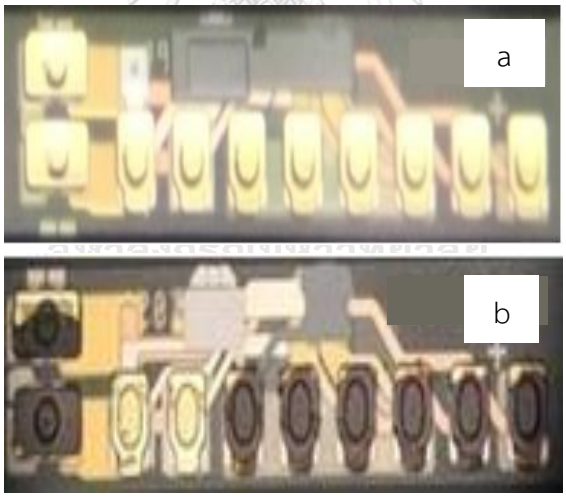

Figure 4.1 (a) The gold electrical contact of slider before lapping, (b) The charged black contamination on the gold electrical contact after lapping.

4.1 Deposited contaminant identification

The EDS spectrum of Cu contacts from electrodepsition test, using sludge from lapping process as electrolyte, were shown in Figure 4.2 (a), (b) and (C), respectively. The major x-ray peaks presented of Cu, together with bismuth (Bi) as majority signal. It can be seen clearly that the black contaminant layers were mostly Bi particles. This result was in consistence with the EDS results performed directly on the slider gold contacts. This Bi contamination came off from Bi-Sn alloy lapping plate material as sliders were wear on their surface. After that, the Bi particles were charged by tribocharging effect during the lapping friction. The electrostatic potential drove the charged Bi particles attracted then deposited on the electrical contacts which connected to the ground to the lapping system. Moreover, the spectrum showed the present of Al. It indicated that Al were polished out from AlTiC substrate to sludge (from Al_2O_3). This caused a complete circuit loop of the electrodeopsition and created the Bi layer coated on the surface of electrode (both Au pads in slider and Cu test specimen). It was also found that this phenomenon can occur as the electrostatic potential increases above 1.5 V.

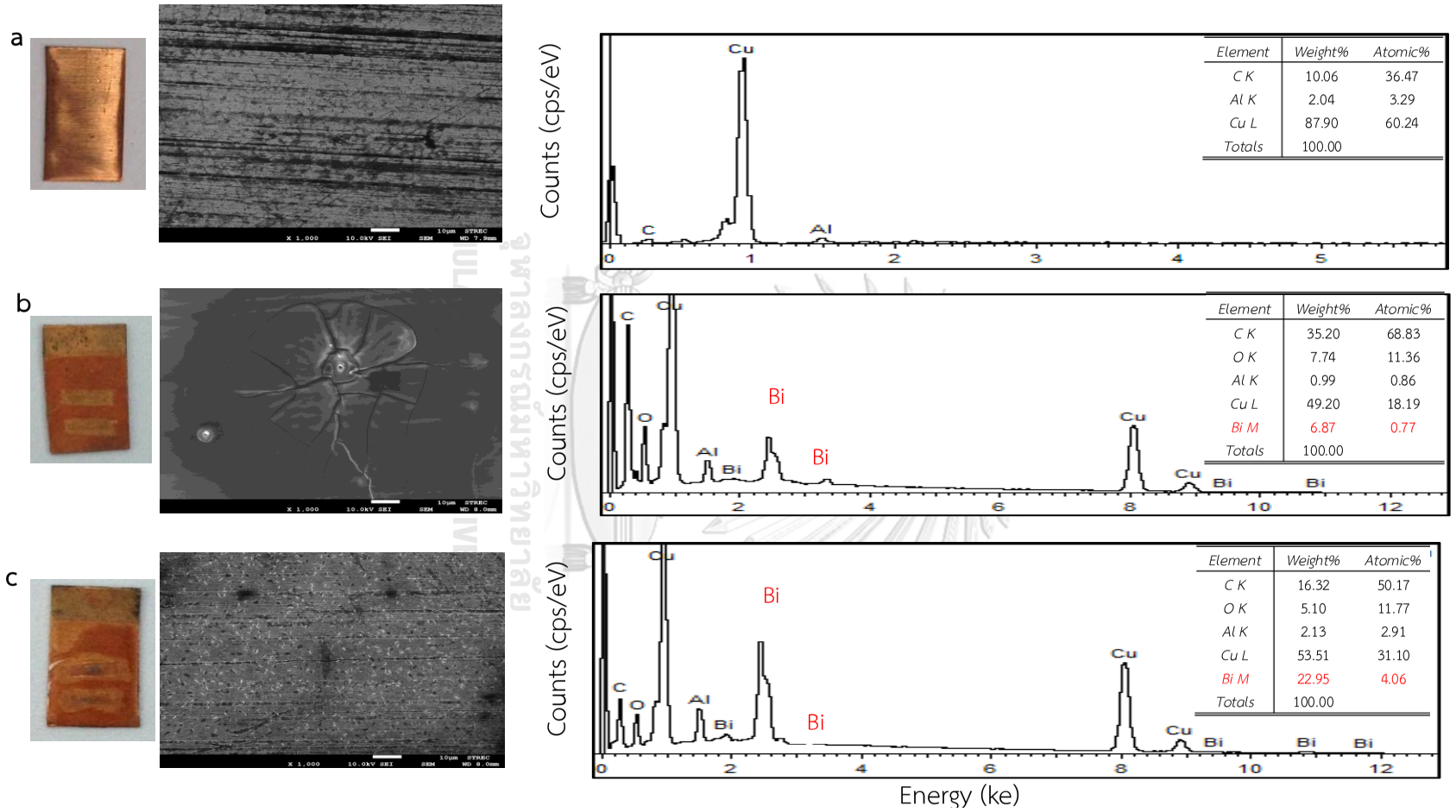

Figure 4.2 EDS spectrum of (a) clean copper contact and (b) copper contact with contamination layer at 2V and (c) copper contact with contamination layer at 4V.

4.2 Surface characterization

The electron micrographs of electroplated Bi particles on copper electrical contacts, using sludge mixed with different surfactants, are shown in Figure 4.3. In this electrodeposition experiment, the voltage between the cathode and anode was set at 1.5 V with the electrode distance about 4 cm. The upper part of the line was covered during electrodeposition test, as reference area (no deposition). The lower part of the line was the exposed surface that had the Bi deposition. Figure 4.3 (a) and (b) showed the clean surface of Cu contact before electroplating and the surface after electrodeposition, using sludge obtained from the lapping process. Obviously, the surface in the deposition zone shown deposited contaminant layer of Bi particles from the sludge. The surface of electrodeposited Cu contacts using sludge mixed with 1 %wt of each surfactant, were then investigated (see Figure 4.3 c-i). From the result, it can be seen clearly that the amount of Bi deposition on the surface was a difference, compared to the deposited surface using pure sludge. The SEM results showed that some surfactants (PEAL, QA and PO) can provide a protection of the surface from Bi particle contamination. Those effective surfactants were chosen for further characterizations for their protective mechanisms and functions.

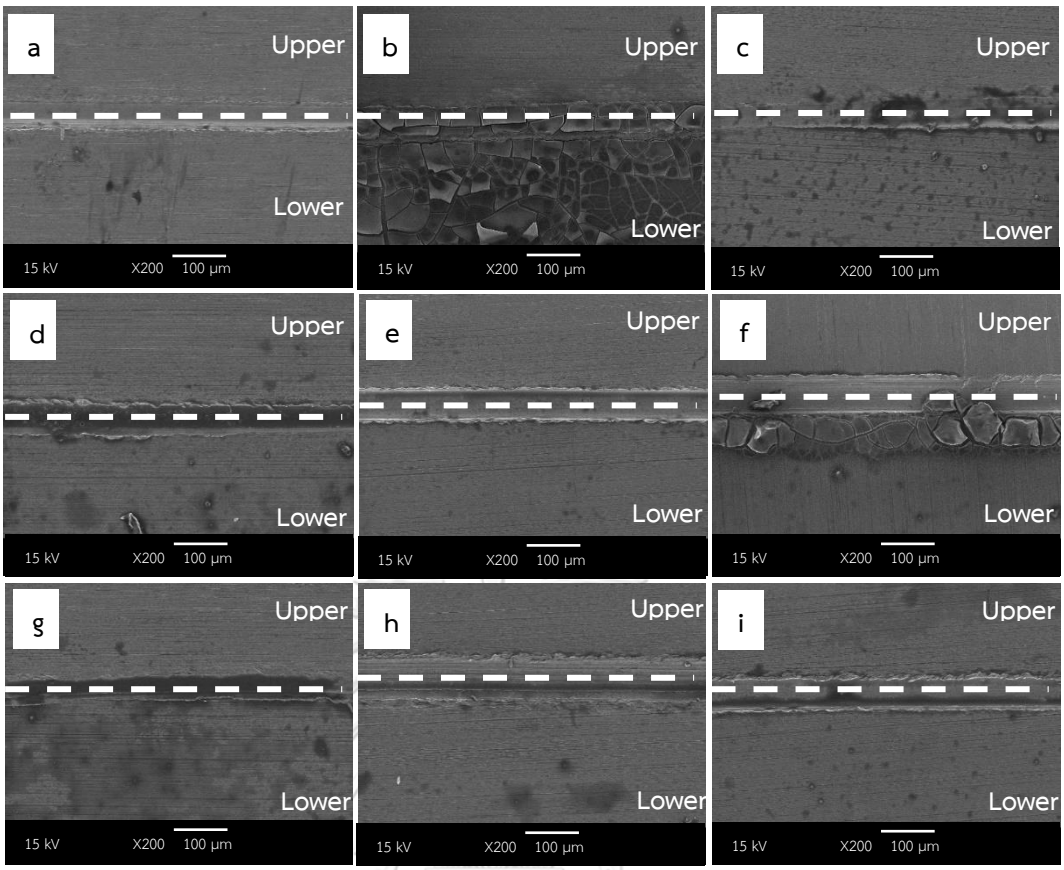

Figure 4.3 SEM of (a) clean copper surface, copper surface after electrodeposition using (b) pure sludge and copper surface after electrodeposition using sludge mixed with (c) EAO, (d) EAL, (e) PEAL, (f) CTAB, (g) AAO, (h) QA and (i) PO

4.3 Characteristics of modified lubricants

For understanding function of surfactant, selected surfactant (PEAL, QA and PO) were investigated for their chemical and physical properties for consideration on their efficiency in modified lubricant and provided the suitable lubricant for slider lapping process.

4.3.1 pH

The pH values of modified lubricant were shown in Table 4.1. It can be seen that all modified lubricants were base because adding surfactant induced slightly changed pH in range between 8.4-8.6. It was not significant. The pH value of SL+QA lubricant was tern to decrease due to ammonium group.

Table 4.1 pH of modified lubricant

Lubricant	The concentration of surfactants					
	0.0 %wt	0.2 %wt	0.4 %wt	0.6 %wt	0.8 %wt	1.0 %wt
SL	8.4	-	-	-	-	-
SL+PEAL	-	8.5	8.5	8.6	8.5	8.5
SL+QA	-	8.5	8.6	8.4	8.3	8.2
SL+PO	-	8.5	8.5	8.4	8.5	8.6

4.3.2 Total base number (TBN)

The TBN value of the PEAL-, PO- and QA- modified lubricant was shown in Table 4.2. TBN value of modified lubricant was increased from 3.72 mg KOH/g to the range 22-24 mg KOH/g when compared with SL. It can be described the adding surfactant provided the basicity from their chemical properties. The TBN value can be defined as the higher TBN was able to neutralize a greater amount of acidic materials for protecting corrosion effect.

Table 4.2 TBN of modified lubricant

Lubricant	The concentration of Surfactants					
	0.0 %wt	0.2 %wt	0.4 %wt	0.6 %wt	0.8 %wt	1.0 %wt
SL	3.72	-	-	-	-	-
SL+PEAL	-	22.7	22.8	23.1	22.7	22.8
SL+QA	-	22.8	23.5	23.0	22.2	22.8
SL+PO	-	22.7	22.9	22.6	22.8	22.8

4.3.3 Conductivity

The conductivity of all three modified lubricants was shown in Table 4.3. It was found that the amount of QA affected on conductivity value due to ammonium ion. So, it increased conductivity value of the modified lubricant as the concentration increased. While adding PEAL and PO into SL affected in decreasing of conductivity. In generally, conductivity of lubricant should be low, in order to avoid the corrosion on the slider head.

Table 4.3 Conductivity of modified lubricant

Lubricant	The concentration of Surfactants					
	0.0 %wt	0.2 %wt	0.4 %wt	0.6 %wt	0.8 %wt	1.0 %wt
SL	126.4	-	-	-	-	-
SL+PEAL	-	108.5	108.3	106.2	102.1	111.0
SL+QA	-	147.2	162.3	187.4	189.8	217.3
SL+PO	-	113.7	116.4	120.9	124.1	118.9

4.3.4 Quasi-static test (QST)

The changed in MRR values of slider in QST can be related to the properties of metal layers on slider surface by many factors such as corrosion effect, lapping, chemical in lubricant, etc. The results from QST are shown in Figure 4.4 and Table 4.4. It was found that the mean values of %ΔMRR were effectively decreased from 2.99 to 0.44 and 2.99 to 1.63, respectively, as the concentration PEAL and QA were increased. On the other hand, the more concentration of PO in the modified lubricant slightly increased %ΔMRR from 1.89 to 2.49. The result can be clarified that the more adding concentration of PEAL and QA led to the modified lubricant that can capable reduce the corrosion effect from the reaction of modified lubricant to slider materials, while PO can efficiently utilize at low concentration. Moreover, the results presented these modified lubricants cased little distribution %ΔMRR of slider that mean they had an anti-corrosion property as an additional function. Therefore, the optimum concentration of each surfactant was obtained as PEAL, QA and PO exhibited the low %ΔMRR at concentration of 1.0, 1.0 and 0.2 %wt, respectively. Then modified lubricants with these optimum concentrations were used in further study.

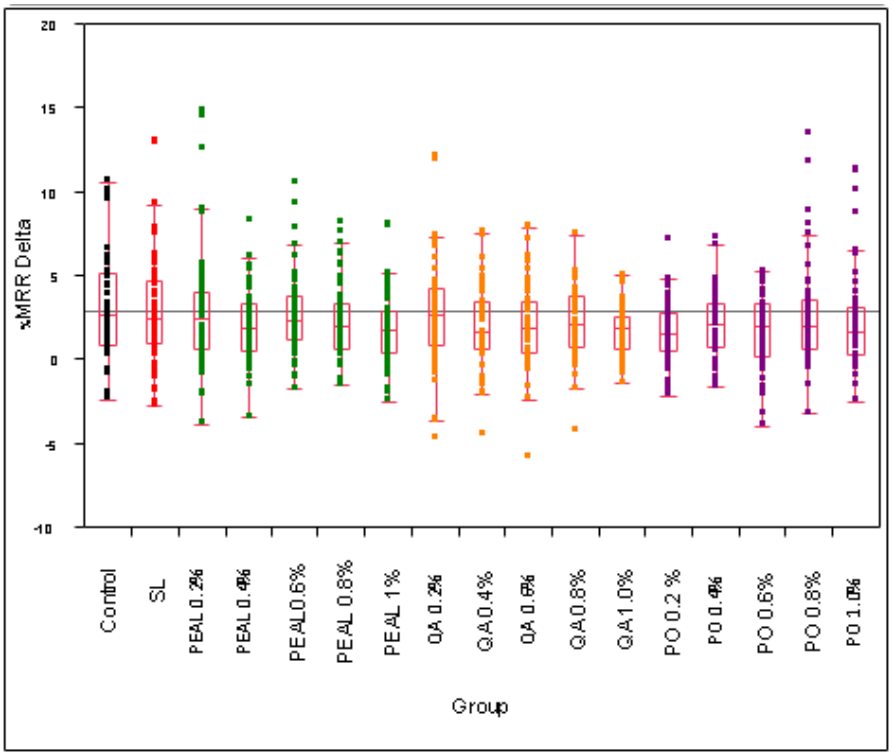

Figure 4.4 %MRR Delta of modified lubricants and standard lubricant (from oneway analysis, JMP program)

Table 4.4 Statistical values of the measured QST parameters

Lubricant		Mean	STD error
Control		3.75	2.96
SL		2.99	2.96
PEAL	$PEAL_{0.2}$	2.92	2.96
	$PEAL_{0.4}$	2.02	2.96
	$PEAL_{0.6}$	2.59	2.96
	$PEAL_{0.8}$	2.18	2.96
	$PEAL_{1}$	0.44	2.96
QA	$QA_{0.2}$	3.48	2.96
	$QA_{0.4}$	2.01	2.98
	$QA_{0.6}$	1.92	2.96
	$QA_{0.8}$	2.33	2.96
	QA_{1}	1.63	2.96
PO	$PO_{0.2}$	1.89	2.96
	$PO_{0.4}$	2.21	2.96
	$PO_{0.6}$	2.14	2.98
	$PO_{0.8}$	2.49	2.96
	PO_{1}	2.40	2.96

*Control is slider bars that did not soaked in lubricant.

4.4 Functional surfactant studies

The studied of the mechanisms and functions of surfactant including the important parameter, CMC of surfactant was investigated and can be referred to the self-assembly of micelle formation of the surfactant-modified lubricants which can indicated the efficiency of contamination protection. CMC can be extracted from the slope changing point of the concentration dependence fluorescence emission curve (see Figure 4.4). Normally, the obtained CMC value in lubricant exhibits higher value than in aqueous solution because the standard lubricant (SL) contains glycol chain. The presence of EG decreases the cohesive energy of the medium, thus increasing the solubility of surfactant in its monomeric form will lead to increase of the CMC [53-58].

The results in Figure 4.5 showed that PEAL reached their CMC values at 0.64 mM (0.04 %wt). Therefore, at 1wt% of working concentration in modified lubricant is much higher than the CMC value of PEAL, PEAL to form the micelle in modified lubricant. The molecular dimension of PEAL micelle which measured from the length of surfactant molecule was predicted about 11.86 Å. In this case, the hydrophilic oxyethylene group of PEAL can reduce the charge of Bi particles. The environment, oxygen source in the reaction media, played as a nucleophile to attack the oxyethylene groups that led to product the acetoxy group, together with reduction the charge of Bi particles. The Bi particles were tended to migrate into the micelles of PEAL, as illustrated in Figure 4.6. Therefore, these micelles can accommodate and protect the growth of Bi layer on surface [59, 60].

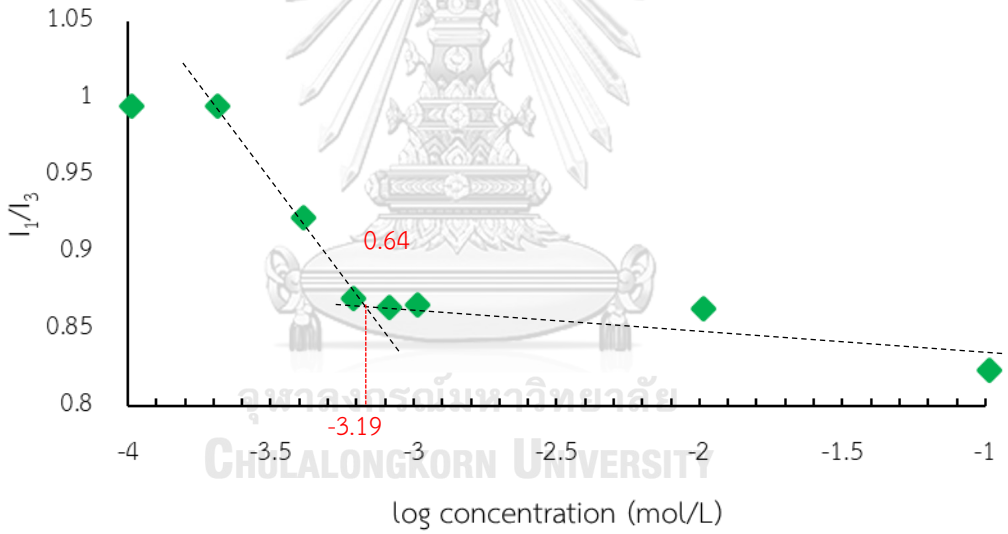

Figure 4.5 Pyrene intensity ratio I_1/I_3 versus log concentration with total surfactant molar concentration for PEAL modified lubricant

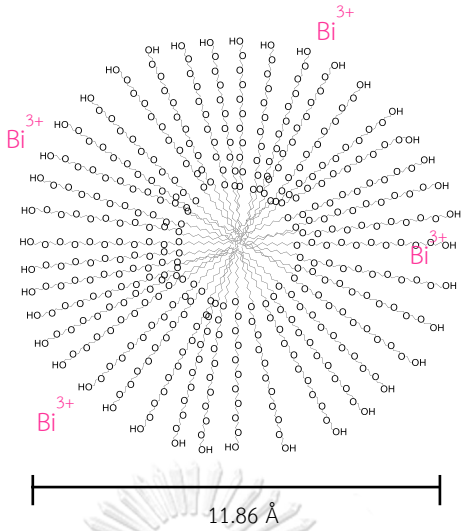

Figure 4.6 Schematic micellization of PEAL

The QA can form micelle at the CMC of about 0.88 mM (0.03 % wt) in glycol lubricant (see Figure 4.7). Consequently, the micelles can be completely formed at 1 %wt of QA concentration. The prediction of molecular dimension was about 79.92 Å. It was found that its molecule exhibited dual ionic part in term of amine ion (cationic ion) and the polyoxyethylene group in QA chain. The association of charged Bi with cationic of QA micelles involved electrostatic interaction that was illustrated in Figure 4.8. Thus, charged Bi was expected to be present near the Stern layer and was not deposit on surface [61].

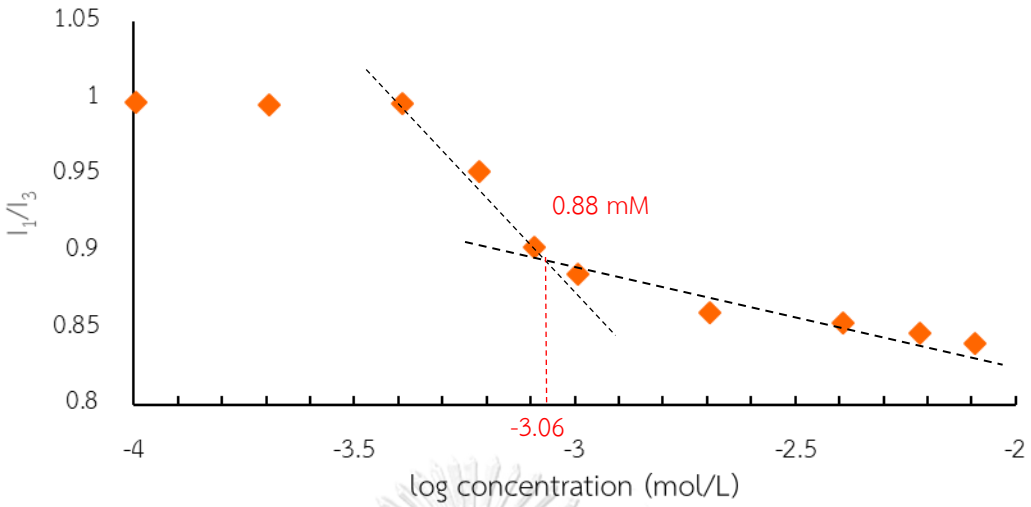

Figure 4.7 Pyrene intensity ratio I_1/I_3 versus log concentration with total surfactant molar concentration for QA modified lubricant

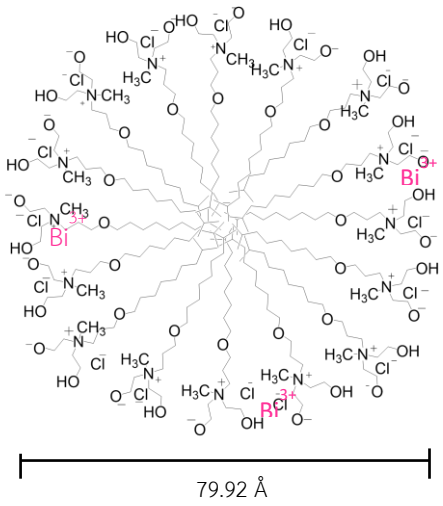

Figure 4.8 Schematic micellization of QA

In case of PO, its CMC was at 4.69 mM (0.52 %wt) (see Figure 4.9). Then, at 0.2 wt% of working concentration in modified lubricant cannot form micelle due to intra- and inter-steric chain repulsions in macromolecules. The molecular size was 34.45 Å. The oxyethylene groups established hydroperoxides with oxygen in environment. Then, the hydroperoxides led to decrease the metal ion to metal [62]. Therefore, PO has 20 ethoxy groups per molecule, the number of decreasing equivalents should be the same order. Hence, PO was able to decrase the charged Bi to the neutral state via oxidation of the oxyethylene groups into hydroperoxides in Figure 4.10. At the same time the surfactant molecules adsorb Bi particles on the surface and prevent the deposited.

Based on all CMC results, we found that PEAL-, QA- and PO-modified lubricants had the potential to prevent the deposited contaminant on the electrical contact surface of the HDD sliders.

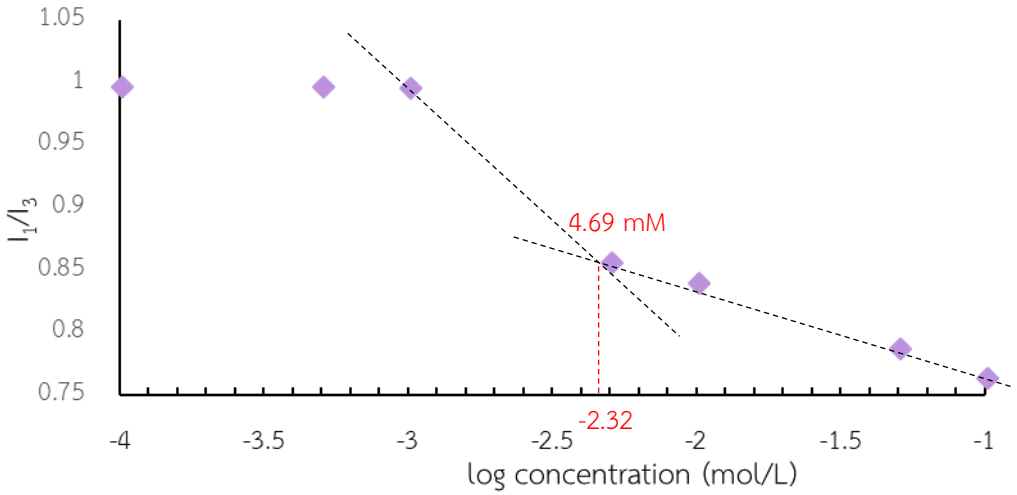

Figure 4.9 Pyrene intensity ratio I_1/I_3 versus log concentration with total surfactant molar concentration for PO modified lubricant

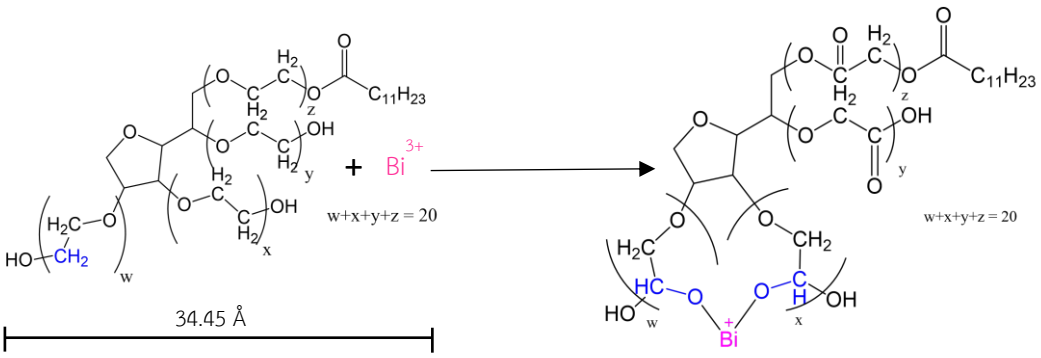

Figure 4.10 Schematic micellization of PO

4.5 Performance of lubricant

4.5.1 Corrosion rate

The $i_{corr,}$ E_{corr} and corrosion rate were the factors that can be used to determine the corrosion of slider from modified lubricants by Potentiodynamic polarization curve. The Tafel extrapolations for all 3 modified lubricants are shown in Figure 4.10. At the intercept of Tafel slope, X is E_{corr} and Y is log i_{corr}. The higher E_{corr}, the more difficult to corrode. Whereas, the higher i_{corr} gives slower corrosion rate. The higher corrosion rate was the faster corrosion. From Figure 4.10 and Table 4.2, the SL showed the highest corrosion rate at 0.15 Å/min which was the fastest corrosion. The 1 %wt of PEAL, 1 %wt of QA and 0.2 %wt of PO obtained corrosion rates about 0.03, 0.07, 0.08 Å/min, respectively. Therefore, 1 %wt of PEAL had the least corrosion effects. Moreover, PEAL-modified lubricant shows E_{corr} at -0.053 V and has the best i_{corr}, compared to others. This is because PEAL is nonionic surfactant that has mild reaction. The corrosion test results concluded that all 3 modified lubricants offer lower corrosion effect than the SL. Thereby, these 3 modified lubricants also provided the anti-corrosion function; additional from the surface contamination protection.

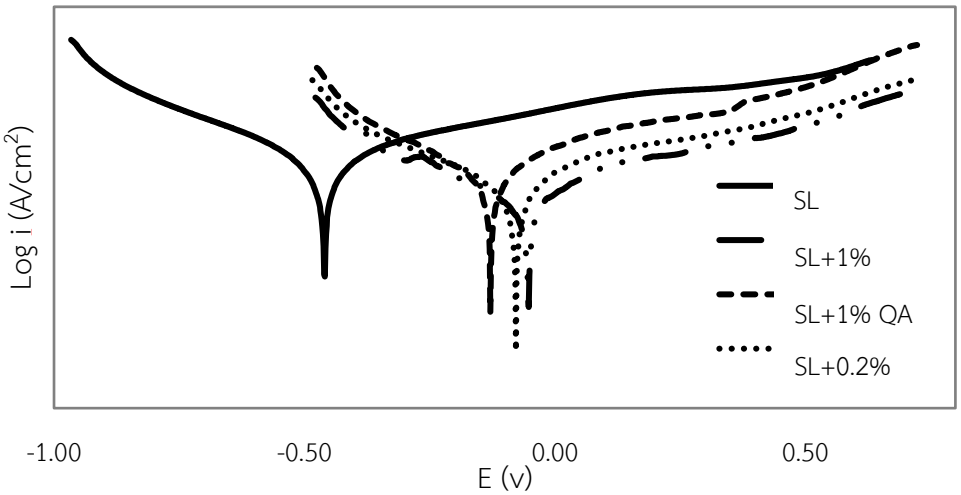

Figure 4.11 Potentiodynamic polarization curve of glycol-based lubricant compared with added surfactant

Table 4.5 Corrosion parameters and lap time of modified lubricant

Lubricant	I_{corr} (nA)	E_{corr} (V)	Corrosion Rate (Å/min)
SL	0.030	-0.460	0.15
SL+ 1%PEAL	0.006	-0.053	0.03
SL+ 1%QA	0.015	-0.128	0.07
SL+ 0.2%PO	0.016	-0.077	0.08

4.5.2 Lap time

The lapping times measured from the actual lapping process with those modified lubricants are shown in Table 4.2. The 0.2 %wt PO modified lubricant gave the shortest lap time because the minor ratio of surfactant was influence to less long chain carbon that related to the least viscosity. It presented the 0.2 %wt PO modified lubricant provided the high material.

Table 4.6 lap time and viscosity of modified lubricant

Lubricant	Lap time (min)	Viscosity (cP)	Average of COF
SL	1.57	20.00	0.0651
SL+ 1%PEAL	2.03	19.60	0.0733
SL+ 1%QA	1.54	19.40	0.0914
SL+ 0.2%PO	1.53	19.00	0.0916

4.5.3 Coefficient of friction

The coefficient of friction (COF) values of modified lubricant slightly increased when compared with SL (see Table 4.6). Therefore, COF of modified lubricants and SL are not different significantly.

Chapter V
Conclusions and Suggestions

In HDD slider lapping process, diamond embedded Bi-Sn alloy lapping plate was used together with functional lubricant to reduce excessive friction side-effects and protect the surface from corrosion. At the stage of final lapping, it was found that some sliders had bismuth particles deposited on gold pads due to electrotribocharging. We found that the threshold voltage for Bi contaminant deposition on Au-electrical contact was about 1.5 V. This contaminant can cause the failure to the HDD. After simulate the lapping process by electroplating of sludge on Cu pad, SEM results indicated that some selected surfactants can help to prevent the surface contamination. Therefore, the selected surfactants such as polyethoxylate alcohol (PEAL), quaternary amines (QA) and polyoxyethylene-(20)-sorbitan monostearate (PO), were considered and investigated to be further used with the standard glycol-based lapping lubricant, in order to protect and reduce bismuth and other the contaminants during lapping process. The results showed that the modified lubricants can help to protect the bismuth deposition on electrical contacts with those functional surfactants. At optimum working concentration of 1 %weight, PEAL creates the micellization due to the partial negative charges of polyoxyethylene group which can balance bismuth charges. The charged bismuth particles were attached to polyoxyethylene groups and became neutral particles. The modified lubricant with QA at 1%wt concentration, can also form micelle and protect the surface deposition by association of charged bismuth particles with the cationic surfactant of QA micelles via electrostatic interaction. Thus, charged bismuth particles were expected to be present near the stern layer. Another surfactant, PO did not form micelle at 0.2 %weight of working concentration in lubricant due to intra- and inter-steric chain repulsions. However, PO protects the surface contaminant deposition by neutralize charge of bismuth particles through the

oxidation of oxyethylene group into acetoxy group and suspend bismuth particles in lubricant.

All the modified lubricants were investigated on their chemical properties and performance. %ΔMRR values of PEAl-, QA- and PO- modified lubricant were measured at concentration of 1.0, 1.0 and 0.2 %wt, respectively. These modified lubricants had minor distribution failure to MRR of slider that mean they had minor influence in case of corrosion. Therefore, these were the working concentrations were used in further study. The corrosion rates of all modified lubricants were almost 300% lower than the standard lubricant, which indicated an anti-corrosion function, as an extra function apart from the surface contamination protection. The actual lapping, viscosity and tribology test confirmed that PEAL, QA and PO can be used as functional surfactant additives in standard lapping lubricant, without introducing additional failure to the lapping process.

Finally, considering overall performance parameters, we propose that QA should be the 1st choice of surfactant that can be used in this surface contamination aspect, follow by PO and PEAL as the 2nd and 3rd alternatives. Another parameter is the price of modified lubricants that need to be considered. The price of standard lubricant is 417.89 baht/liter, whereas the price of PEAL-, QA- and PO-modified lubricant are 424.59, 419.43 and 417.96 baht/liter, respectively. It indicates the adding surfactant lightly increase the price but efficiency of modified lubricants is more function.

The suggestion for future work

Combination of surfactant and corrosion inhibiter are required for lapping optimization in order to deliver best lapping result and performance.

REFERENCES

1. Totten GE. Tribology of Hard Disk Drives — Magnetic. In: 2, editor. HANDBOOK of LUBRICATION and TRIBOLOGY. Taylor & Francis Group, LLC ed2006.
2. Wang Y, Yan F, Jia Q, Wang Q. Quantitative structure-property relationship for critical micelles concentration of sugar-based surfactants using norm indexes. Journal of Molecular Liquids. 2018;253:205-10.
3. Mu G, Li X. Inhibition of cold rolled steel corrosion by Tween-20 in sulfuric acid: Weight loss, electrochemical and AFM approaches. Journal of Colloid and Interface Science. 2005;289(1):184-92.
4. Zhu W, Zhang K, Chen Y. Block copolymer micelles as carriers of transition metal ions Y(III) and Cu(II) and gelation thereof. Polymer. 2014;55(24):6232-8.
5. Singh T, Mitra S. Fluorimetric studies on the binding of 4-(dimethylamino) cinnamic acid with micelles and bovine serum albumin2008. 1063-70 p.
6. Privé GG. Detergents for the stabilization and crystallization of membrane proteins. Methods. 2007;41(4):388-97.
7. Nazeera Banu VR, Rajendran S, Senthil Kumaran S. Investigation of the inhibitive effect of Tween 20 self assembling nanofilms on corrosion of carbon steel. Journal of Alloys and Compounds. 2016;675:139-48.
8. Oshiki M. Review of perpendicular magnetic recording research at Fujitsu. Journal of Magnetism and Magnetic Materials. 2012;324(3):351-4.
9. Atsumi T. Minimization of unobservable oscillation in repeatable run-out for magnetic-head positioning system of hard disk drives. Mechatronics. 2017;44:24-31.
10. Wood R. Future hard disk drive systems. Journal of Magnetism and Magnetic Materials. 2009;321(6):555-61.
11. Gruhn M. Forensic limbo: Towards subverting hard disk firmware bootkits. Digital Investigation. 2017;23:138-50.
12. Coughlin TM. Chapter 2 - Fundamentals of Hard Disk Drives. Digital Storage in Consumer Electronics. Burlington: Newnes; 2008. p. 25-51.

13. Jiang M, Hao S, Komanduri R. On the advanced lapping process in the precision finishing of thin-film magnetic recording heads for rigid disc drives. Applied Physics A. 2003;77(7):923-32.
14. Jessada Wannasin CS, Benjie L. Fernandez, Santoso Tan, Prakasit Sukasem. Handbook of the Final Lapping Process2013.
15. Bart JCJ, Gucciardi E, Cavallaro S. 12 - Biolubricant product groups and technological applications. Biolubricants: Woodhead Publishing; 2013. p. 565-711.
16. Bart JCJ, Gucciardi E, Cavallaro S. 2 - Principles of lubrication. Biolubricants: Woodhead Publishing; 2013. p. 10-23.
17. Bart JCJ, Gucciardi E, Cavallaro S. 3 - Lubricants: properties and characteristics. Biolubricants: Woodhead Publishing; 2013. p. 24-73.
18. Nakama Y. Chapter 15 - Surfactants. Cosmetic Science and Technology. Amsterdam: Elsevier; 2017. p. 231-44.
19. Prietoblanco M, Lopezmahia P, Muniateguilorenzo S, Pradarodriguez D. Determination of Surfactants in Cosmetics2007. 291-322 p.
20. Miyake M, Yamashita Y. Molecular Structure and Phase Behavior of Surfactants2017. 389-414 p.
21. Free ML. Chapter 13 - The Use of Surfactants to Enhance Particle Removal from Surfaces. Developments in Surface Contamination and Cleaning (Second Edition). Oxford: William Andrew Publishing; 2016. p. 595-626.
22. Bhattarai A, Ajaya. The solution behaviour of a surfactant in mixed solvent media2012.
23. Ribeiro AM, Amaral C, Veiga F, Figueiras A. Chapter 8 - Polymeric micelles as a versatile tool in oral chemotherapy A2 - Grumezescu, Alexandru Mihai. Design and Development of New Nanocarriers: William Andrew Publishing; 2018. p. 293-329.
24. Piñeiro L, Novo M, Al-Soufi W. Fluorescence emission of pyrene in surfactant solutions. Advances in Colloid and Interface Science. 2015;215:1-12.
25. Consoli GML, Granata G, Geraci C. Chapter 3 - Calixarene-based micelles: Properties and applications A2 - Grumezescu, Alexandru Mihai. Design and

Development of New Nanocarriers: William Andrew Publishing; 2018. p. 89-143.

26. Assumpção Pereira-da-Silva M, Ferri FA. 1 - Scanning Electron Microscopy A2 - Róz, Alessandra L. Da. In: Ferreira M, Leite FdL, Oliveira ON, editors. Nanocharacterization Techniques: William Andrew Publishing; 2017. p. 1-35.
27. Zhang L, Shi W, Zhang B. A review of electrocatalyst characterization by transmission electron microscopy. Journal of Energy Chemistry. 2017;26(6):1117-35.
28. Yoshida A, Kaburagi Y, Hishiyama Y. Chapter 5 - Scanning Electron Microscopy A2 - Inagaki, Michio. In: Kang F, editor. Materials Science and Engineering of Carbon: Butterworth-Heinemann; 2016. p. 71-93.
29. Henning S, Adhikari R. Chapter 1 - Scanning Electron Microscopy, ESEM, and X-ray Microanalysis A2 - Thomas, Sabu. In: Thomas R, Zachariah AK, Mishra RK, editors. Microscopy Methods in Nanomaterials Characterization: Elsevier; 2017. p. 1-30.
30. Inkson BJ. 2 - Scanning electron microscopy (SEM) and transmission electron microscopy (TEM) for materials characterization. Materials Characterization Using Nondestructive Evaluation (NDE) Methods: Woodhead Publishing; 2016. p. 17-43.
31. Abd Mutalib M, Rahman MA, Othman MHD, Ismail AF, Jaafar J. Chapter 9 - Scanning Electron Microscopy (SEM) and Energy-Dispersive X-Ray (EDX) Spectroscopy. Membrane Characterization: Elsevier; 2017. p. 161-79.
32. Waters JC, Wittmann T. Chapter 1 - Concepts in quantitative fluorescence microscopy. In: Waters JC, Wittman T, editors. Methods in Cell Biology. 123: Academic Press; 2014. p. 1-18.
33. Wayne R. Chapter 11 - Fluorescence Microscopy. Light and Video Microscopy (Second Edition). San Diego: Academic Press; 2014. p. 205-17.
34. Wolf DE. Chapter 4 - Fundamentals of Fluorescence and Fluorescence Microscopy. In: Sluder G, Wolf DE, editors. Methods in Cell Biology. 114: Academic Press; 2013. p. 69-97.

35. Wikipedia. Fluorescence microscope 2018 [cited 2018 22 June]. Available from: https://en.wikipedia.org/wiki/Fluorescence_microscope.
36. Revie RWaU, H.H. Corrosion and Corrosion Control An Introduction to Corrosion Science and Engineering. ed t, editor.
37. Foster LS. Corrosion and corrosion control: An introduction to corrosion science and engineering (Uhlig, Herbert H.). Journal of Chemical Education. 1964;41(2):A126.
38. Roy D. 3 - Electrochemical techniques and their applications for chemical mechanical planarization (CMP) of metal films A2 - Babu, Suryadevara. Advances in Chemical Mechanical Planarization (CMP): Woodhead Publishing; 2016. p. 47-89.
39. Makhlouf ASH, Herrera V, Muñoz E. Chapter 6 - Corrosion and protection of the metallic structures in the petroleum industry due to corrosion and the techniques for protection. Handbook of Materials Failure Analysis: Butterworth-Heinemann; 2018. p. 107-22.
40. Hasan BO. Galvanic corrosion of carbon steel–brass couple in chloride containing water and the effect of different parameters. Journal of Petroleum Science and Engineering. 2014;124:137-45.
41. Prakash S. Chapter 4 - From Rheology to Tribology: Applications of Tribology in Studying Food Oral Processing and Texture Perception A2 - Ahmed, J. In: Ptaszek P, Basu S, editors. Advances in Food Rheology and Its Applications: Woodhead Publishing; 2017. p. 65-86.
42. Lenard JG. 9 - Tribology. Primer on Flat Rolling (Second Edition). Oxford: Elsevier; 2014. p. 193-266.
43. McKeen LW. 2 - Introduction to the Tribology of Plastics and Elastomers. Fatigue and Tribological Properties of Plastics and Elastomers (Third Edition): William Andrew Publishing; 2016. p. 27-44.
44. Liu Y, Hu J, Zhong M, Xu W. A novel, simple and rapid method for the detection of melamine from milk based on tribology measurements. Tribology International. 2018;119:66-72.

45. Gao Y, Ma L, Guo D, Luo J. Ultra-low friction achieved by diluted lactic acid solutions. RSC Advances. 2014;4(55):28860-4.
46. Cui F, Wang L, Cui Y. Determination of bismuth in pharmaceutical products using methyltriphenylphosphonium bromide as a molecular probe by resonance light scattering technique. Journal of Pharmaceutical and Biomedical Analysis. 2007;43(3):1033-8.
47. Didi MA, Sekkal AR, Villemin D. Cloud-point extraction of bismuth (III) with nonionic surfactants in aqueous solutions. Colloids and Surfaces A: Physicochemical and Engineering Aspects. 2011;375(1):169-77.
48. Mokhtari B, Pourabdollah K. Emulsion liquid membrane for selective extraction of Bi(III). Chinese Journal of Chemical Engineering. 2015;23(4):641-5.
49. Shubha HN, Venkatesha TV, Pavithra MK, Punith Kumar MK. Surface modification of mild steel by a self-assembled cetyl-trimethyl ammonium bromide (CTAB) monolayer: Evaluation of its corrosion protection property. Progress in Organic Coatings. 2016;90:267-76.
50. Ponzoni C, Cannio M, Rosa R, Leonelli C. Stabilization of bismuth ferrite suspensions in aqueous medium with sodium polyacrylate characterized by different molecular weights. Materials Chemistry and Physics. 2015;149-150:246-53.
51. Bandyopadhyay P, Ghosh AK. Reversible Fluorescence Quenching by Micelle Selective Benzophenone-Induced Interactions between Brij Micelles and Polyacrylic Acids: Implications for Chemical Sensors. The Journal of Physical Chemistry B. 2010;114(35):11462-7.
52. Nanotechnology TaI. Tribometer - CETR - UMT-2 2015 [Available from: https://www.tint.fs.uni-lj.si/en/equipment/tribology/2015031210295737/Tribometer%20-%20CETR%20-%20UMT-2/.
53. Carnero Ruiz C, Molina-Bolívar J, Aguiar J, MacIsaac G, Moroze S, Palepu R. Effect of ethylene glycol on the thermodynamic and micellar properties of Tween 20. Colloid and Polymer Science. 2003;281(6):531-41.

54. Yan J, Wang D, Bu F, Yang FF. Investigation of the Thermodynamic Properties of the Cationic Surfactant CTAC in EG + Water Binary Mixtures. Journal of Solution Chemistry. 2010;39(10):1501-8.
55. Nagarajan R, Wang C-C. Theory of Surfactant Aggregation in Water/Ethylene Glycol Mixed Solvents. Langmuir. 2000;16(12):5242-51.
56. Akhter MS, Alawi SM. Aggregation of ionic surfactants in formamide. Colloids and Surfaces A: Physicochemical and Engineering Aspects. 2000;173(1):95-100.
57. Obradović S, Poša M. The influence of the structure of selected Brij and Tween homologues on the thermodynamic stability of their binary mixed micelles. The Journal of Chemical Thermodynamics. 2017;110:41-50.
58. Rodrigues OMS, Peres AEC, Martins AH, Pereira CA. Kaolinite and hematite flotation separation using etheramine and ammonium quaternary salts. Minerals Engineering. 2013;40:12-5.
59. Dai Y, Song Y. Facile synthesis and shape control of bismuth nanoflowers induced by surfactants. Chemical Physics Letters. 2014;591:126-9.
60. Sakai T, Alexandridis P. Mechanism of Gold Metal Ion Reduction, Nanoparticle Growth and Size Control in Aqueous Amphiphilic Block Copolymer Solutions at Ambient Conditions. The Journal of Physical Chemistry B. 2005;109(16):7766-77.
61. Ahmad N, Kumar P, Hashmi AA, Khan Z. Effect of cationic micelles of cetytrimethylammonium bromide on the oxidation of thiourea by permanganate. Colloids and Surfaces A: Physicochemical and Engineering Aspects. 2008;315(1):226-31.
62. Premkumar T, Kim D, Lee K, Geckeler K. Polysorbate 80 as a Tool: Synthesis of Gold Nanoparticles2007. 888-93 p.

APPENDIX

1. The obtained CMC values in solution and of modified lubricants were shown in Table A-1.

Table A-1 CMC of surfactants

Surfactant	CMC in aqueous (mM)	CMC in standard lubricant (mM)
SC	0.24	0.64
SF	0.14	0.88
SG	0.054	4.69

2. Calculation CMC from mM to %wt

$$c = \frac{\% \times 10 \times D}{MW}$$

Where c = concentration (mol/l)

% = presentation of solution (%wt)

D = density of solution (g/cm^3)

MW = molecular weight of solute

3. CMC of surfactant PEAL

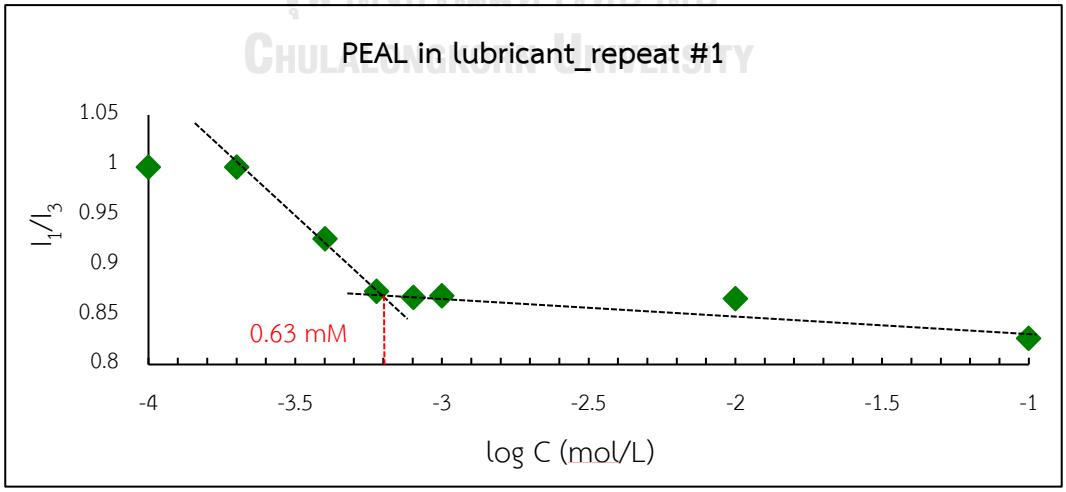

Figure A-1 Pyrene intensity ratio I_1/I_3 versus log concentration with total surfactant molar concentration for PEAL modified lubricant in 1st repeat.

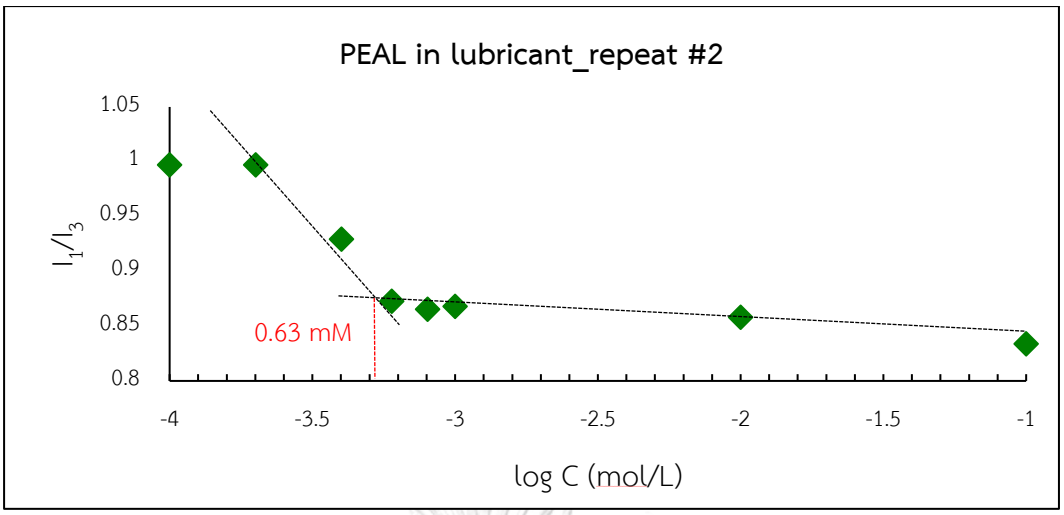

Figure A-2 Pyrene intensity ratio I_1/I_3 versus log concentration with total surfactant molar concentration for PEAL modified lubricant in 2nd repeat.

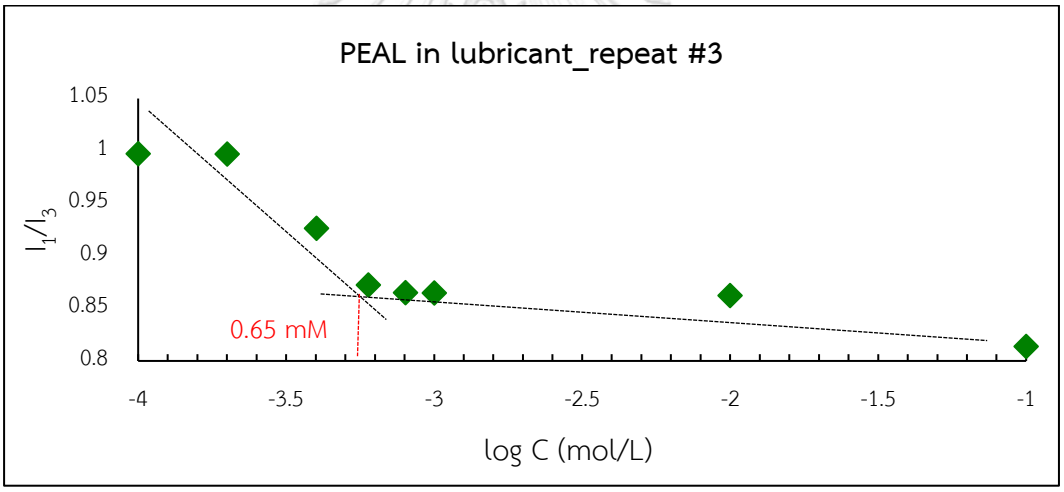

Figure A-3 Pyrene intensity ratio I_1/I_3 versus log concentration with total surfactant molar concentration for PEAL modified lubricant in 3rd repeat.

Table A-2 Result CMC of PEAL in lubricant

Repeat	Log C (mol/L)	CMC (mM)
1	-3.2	0.63
2	-3.2	0.63
3	-3.19	0.65
Average	-3.19	0.64

4. **CMC of surfactant QA**

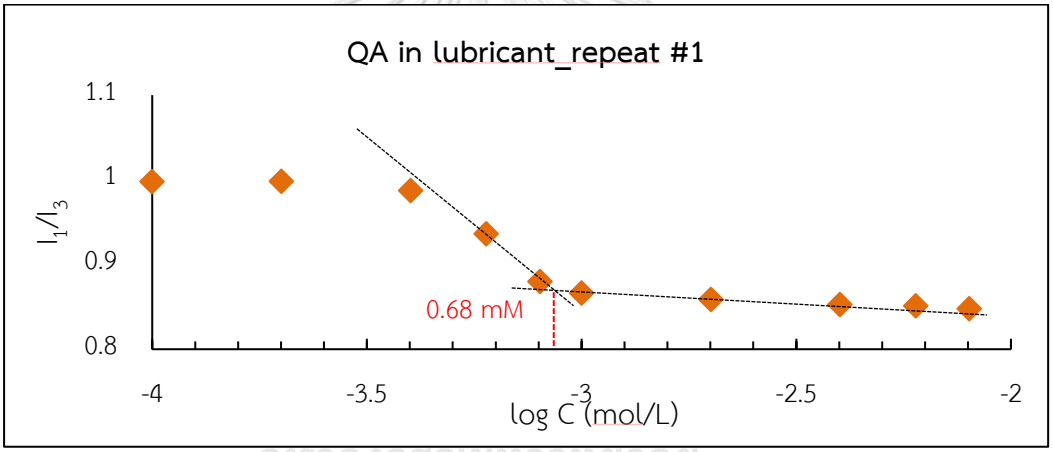

Figure A-4 Pyrene intensity ratio I_1/I_3 versus log concentration with total surfactant molar concentration for QA modified lubricant in 1st repeat.

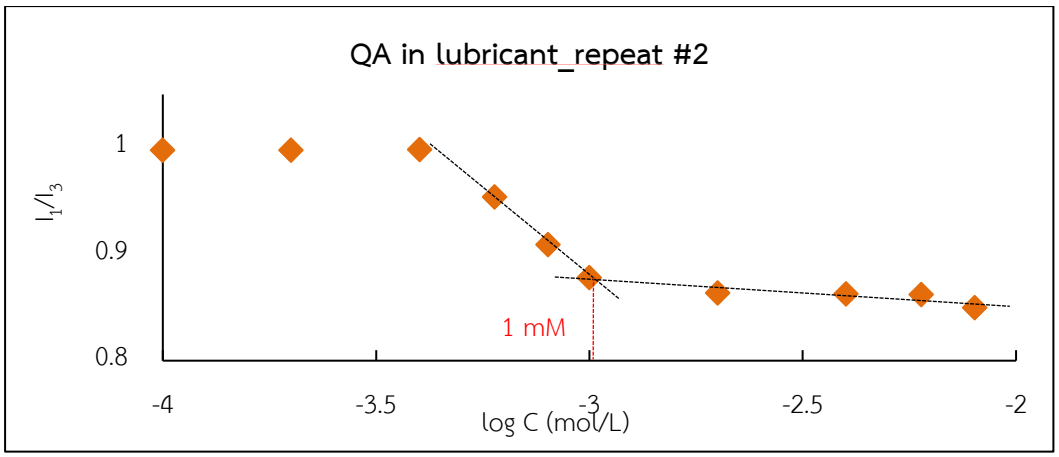

Figure A-5 Pyrene intensity ratio I_1/I_3 versus log concentration with total surfactant molar concentration for QA modified lubricant in 2nd repeat.

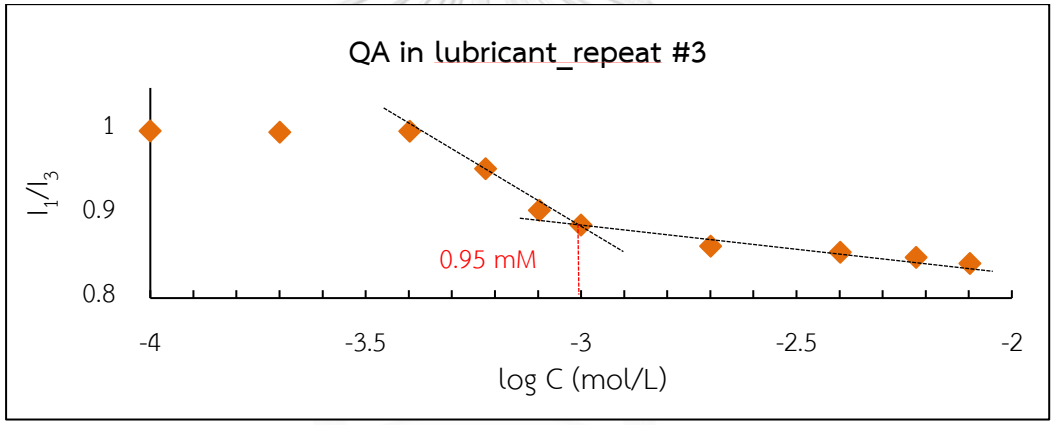

Figure A-6 Pyrene intensity ratio I_1/I_3 versus log concentration with total surfactant molar concentration for QA modified lubricant in 3rd repeat.

Table A-3 Result CMC of QA in lubricant

Repeat	Log C (mol/L)	CMC (mM)
1	-3.17	0.68
2	-3.0	1.00
3	-3.02	0.95
Average	-3.06	0.88

5. CMC of surfactant PO

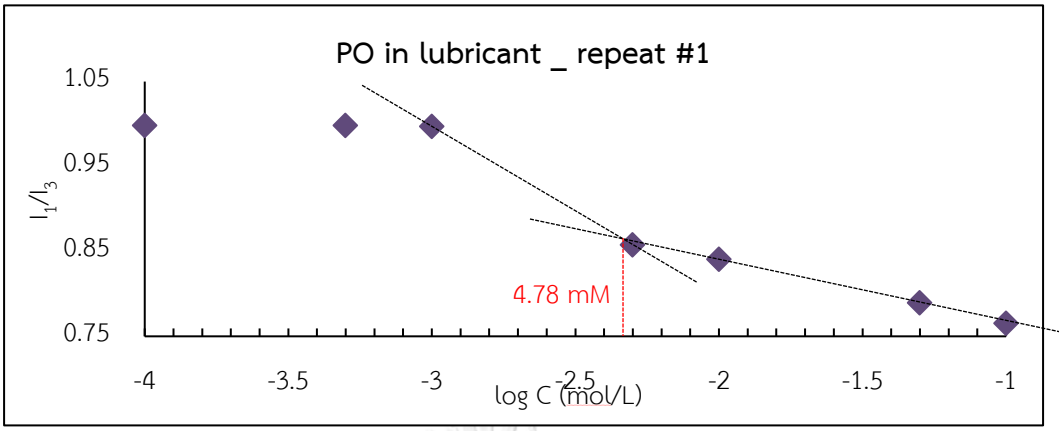

Figure A-7 Pyrene intensity ratio I_1/I_3 versus log concentration with total surfactant molar concentration for PO modified lubricant in 1st repeat.

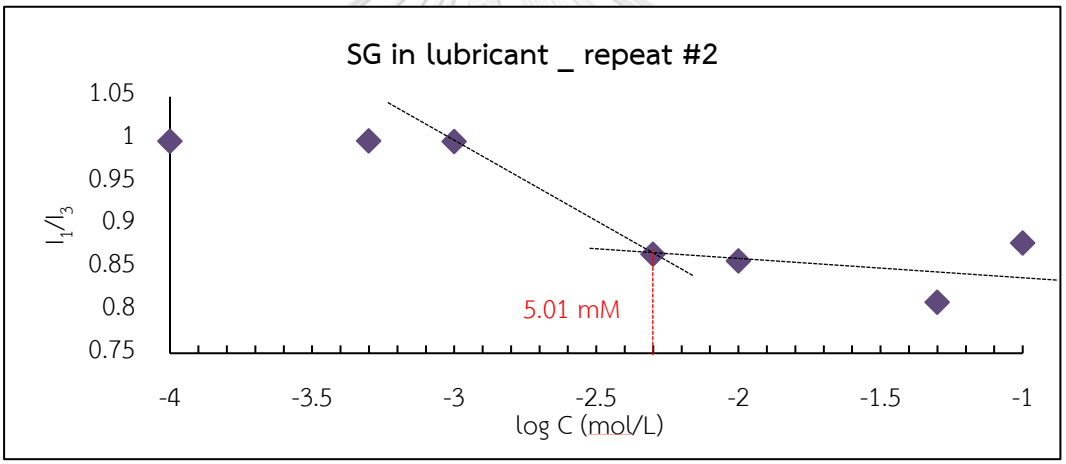

Figure A-8 Pyrene intensity ratio I_1/I_3 versus log concentration with total surfactant molar concentration for PO modified lubricant in 2nd repeat.

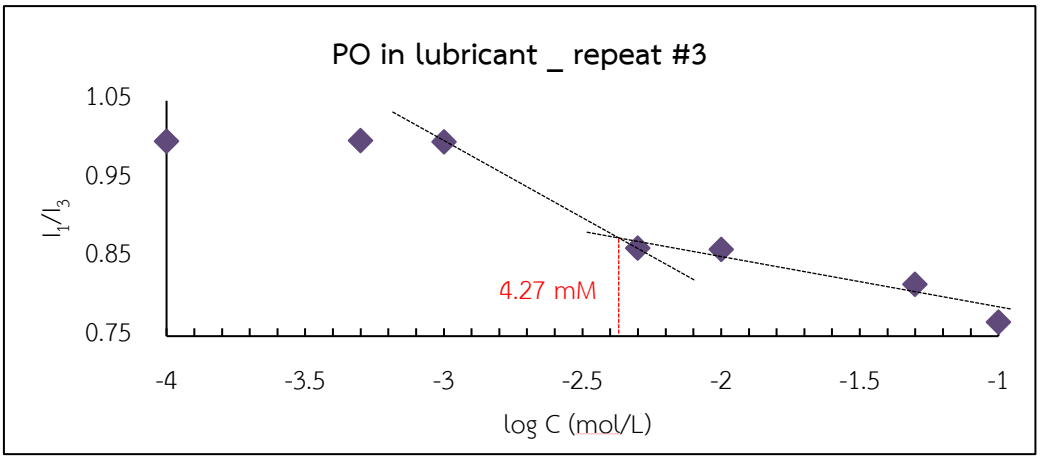

Figure A-9 Pyrene intensity ratio I_1/I_3 versus log concentration with total surfactant molar concentration for PO modified lubricant in 3rd repeat.

Table A-4 Result CMC of PO in lubricant

Repeat	Log C (mol/L)	CMC (mM)
1	-2.32	4.78
2	-2.30	5.01
3	-2.37	4.27
Average	-2.33	4.69

6. The table exhibit all physical and performant properties of working modified lubricant

Table A-5 Physical and performant properties of modified lubricants

Property	SL	$SL+PEAL_1$	$SL+QA_1$	$SL+PO_{0.2}$
EG	93.126	92.126	92.126	92.926
Additives	6.882	6.882	6.882	6.882
Surfactant PEAL	-	1.0	-	-
Surfactant QA	-	-	1.0	-
Surfactant PO	-	-	-	0.2
pH	8.4	8.5	8.2	8.5
TBN (mg KOH/g)	3.72	22.76	22.98	22.71
conductivity	126.4	105.7	187.4	113.7
Lap time (min)	1.58	2.30	1.56	1.55
Corrosion Rate (Å/min)	0.15	0.03	0.07	0.08
Viscosity (cP)	20	19.6	19.4	19.0
Price (THB)	417.89 /L	424.59/L	419.43 /L	417.96 /L

VITA

Miss Chuenkamol Khongphow was born on 7 September, 1991 in Phra Nakhon si Ayutthaya, Thailand. She graduated with a Bachelor's Degree of Science and Technology, major in Chemistry from Thammasat University in 2014. She continued her study in Petrochemistry and Polymer Science Program, faculty of science, Chulalongkorn University in 2015. During her graduate studied, she received a Chulalongkorn University Graduate School Thesis Grant from Chulalongkorn University. She has completed her study leading to a Master's Degree in Petrochemistry and Polymer Science Program in 2018.

Her present address is 22 Moo 7, Thainoi, Bangban, Phra nakhon si Ayutthaya, Thailand 10400. Her email is Khongphow.c@gmail.com